

Recent Advances in Path Integral Control for Trajectory Optimization: An Overview in Theoretical and Algorithmic Perspectives

Muhammad Kazim, JunGee Hong, Min-Gyeom Kim and Kwang-Ki K. Kim*

Abstract—This paper presents a tutorial overview of path integral (PI) control approaches for stochastic optimal control and trajectory optimization. We concisely summarize the theoretical development of path integral control to compute a solution for stochastic optimal control and provide algorithmic descriptions of the cross-entropy (CE) method, an open-loop controller using the receding horizon scheme known as the model predictive path integral (MPPI), and a parameterized state feedback controller based on the path integral control theory. We discuss policy search methods based on path integral control, efficient and stable sampling strategies, extensions to multi-agent decision-making, and MPPI for the trajectory optimization on manifolds. For tutorial demonstrations, some PI-based controllers are implemented in MATLAB and ROS2/Gazebo simulations for trajectory optimization. The simulation frameworks and source codes are publicly available at [the github page](#).

Index Terms—Stochastic optimal control, trajectory optimization, Hamilton-Jacobi-Bellman equation, Feynman-Kac formula, path integral, variational inference, KL divergence, importance sampling, model predictive path integral control, policy search, policy improvement with path integrals, planning on manifolds.

I. INTRODUCTION

Trajectory optimization for motion or path planning [1]–[3] is a fundamental problem in autonomous systems [4]–[6]. Several requirements must be simultaneously considered for autonomous robot motion, path planning, navigation, and control. Examples include the specifications of mission objectives, examining the certifiable dynamical feasibility of a robot, ensuring collision avoidance, and considering the internal physical and communication constraints of autonomous robots.

In particular, generating an energy-efficient and collision-free safe trajectory is of the utmost importance during the process of autonomous vehicle driving [7]–[9], autonomous racing drone [10]–[12], unmanned aerial vehicles [13], electric vertical take-off and landing (eVTOL) urban air mobility (UAM) [14]–[16], missile guidance [17], [18], space vehicle control, and satellite attitude trajectory optimization [19]–[23].

From an algorithmic perspective, the complexity of motion planning is NP-complete [24]. Various computational methods have been proposed for motion planning, including sampling-based methods [25], [26], nonlinear programming (NLP) [27],

The authors are with the department of electrical and computer engineering at Inha University, Incheon 22212, Republic of Korea.

M. Kazim is a postdoctoral fellow affiliated with the ICT-Future Vehicle Convergence Education & Research Center at Inha University.

*Corresponding author (Email: kwangki.kim@inha.ac.kr)

This research was supported by the Basic Science Research Program through the National Research Foundation of Korea (NRF) funded by the Ministry of Education (NRF-2022R1F1A1076260).

[28], sequential convex programming (SCP) [29]–[32], differential dynamic programming (DDP) [33]–[40], hybrid methods [41], and differential-flatness-based optimal control [42], [43].

Optimization methods can explicitly perform safe and efficient trajectory generation for path and motion planning. The two most popular optimal path and motion planning methods for autonomous robots are gradient- and sampling-based methods for trajectory optimization. The former frequently assumes that the objective and constraint functions in a given planning problem are differentiable and can rapidly provide a locally optimal smooth trajectory [44]. However, numerical and algorithmic computations of derivatives (gradient, Jacobian, Hessian, etc.) are not stable in the worst case; preconditioning and prescaling must be accompanied by and integrated into the solvers. In addition, integrating the outcomes of perception obtained from exteroceptive sensors such as LiDARs and cameras into collision-avoidance trajectory optimization requires additional computational effort in dynamic and unstructured environments.

Sampling-based methods for trajectory generation do not require function differentiability. Therefore, they are more constructive than the former gradient-based optimization methods for modelling obstacles without considering their shapes in the constrained optimization for collision-free path planning [26], [45]. In addition, sampling-based methods naturally perform explorations, thereby avoiding the local optima. However, derivative-free-sampling-based methods generally produce coarse trajectories with zigzagging and jerking movements. For example, rapidly exploring random trees (RRT) and probabilistic roadmap (PRM) methods generate coarse trajectories [6], [25], [46], [47]. To mitigate the drawbacks of gradient- and sampling-based methods while maintaining their advantages, a hybrid method that combines them can be considered, as proposed in [48]–[51].

Several open-source off-the-shelf libraries are available for implementing motion planning and trajectory optimization, which include Open Motion Planning Library (OMPL) [52], Stochastic Trajectory Optimization for Motion Planning (STOMP) [53], Search-Based Planning Library (SBPL) [54], And Covariant Hamiltonian Optimization for Motion Planning (CHOMP) [55].

The path integral (PI) for stochastic optimal control, which was first presented in [56], is another promising approach for sampling-based real-time optimal trajectory generation. In the path integral framework, the stochastic optimal control

associated with trajectory optimization is transformed into a problem of evaluating a stochastic integral, for which Monte Carlo importance sampling methods are applied to approximate the integral. It is also closely related to the cross-entropy method [57] for stochastic optimization and model-based reinforcement learning [58] for decision making. The use of path integral control has recently become popular with advances in high-computational-capability embedded processing units [59] and efficient Monte Carlo simulation techniques [60], [61].

There are several variations of the PI control framework. The most widely used method in robotics and control applications is the model predictive path integral (MPPI) control, which provides a derivative-free sampling-based framework to solve finite-horizon constrained optimal control problems using predictive model-based random rollouts in path-integral approximations [59], [62]–[64]. However, despite its popularity, the performance and robustness of the MPPI are degraded in the presence of uncertainties in the simulated predictive model, similar to any other model-based optimal control method. To take the plant-model mismatches of simulated rollouts into account [65], [66], adaptive MPPI [67], learning-based MPPI [68]–[70] and tube-based MPPI [71], uncertainty-averse MPPI [72], fault-tolerant MPPI [73], safety-critical MPPI using control barrier function (CBF) [74]–[76], and covariance steering MPPI [77] have been proposed. Risk-aware MPPI based on the conditional value-at-risk (CVaR) have also been investigated for motion planning with probabilistic estimation uncertainty in partially known environments [78]–[81].

The proportional-integral (PI) control framework can also be combined with parametric and nonparametric policy search methods and improvements. For example, RRT is used to guide PI control for exploration [82] and PI control is used to guide policy searches for open-loop control [83], parameterized movement primitives [84], [85], and feedback control [58], [86], [87]. To smoothen the sampled trajectories generated from the PI control, gradient-based optimization, such as DDP, is combined with MPPI [88], regularized policy optimization based on the cross-entropy method is used [89], and it is also suggested to smooth the resulting control sequences using a sliding window [90], [91] and a Savitzky-Golay filter (SGF) [63], [92] and introducing an additional penalty term corresponding to the time derivative of the action [93].

PI control is related to several other optimal control and reinforcement learning strategies. For example, variational methods of path integral optimal control are closely related to entropy-regularized optimal control [94], [95] and maximum entropy RL (MaxEnt RL) [85], [96]. The path integral can be considered as a probabilistic inference for stochastic optimal control [97]–[99] and reinforcement learning [100], [101].

One of the most important technical issues in the practical application of path integral control is the sampling efficiency. Various importance sampling strategies have been suggested for rollouts in predictive optimal control. Several importance sampling (AIS) algorithms exist [102], [103] with different performance costs and benefits, as surveyed in [104]. AIS procedures are considered within the optimal control [61],

[105] and MPPI control [106]. In addition to the AIS algorithms, learned importance sampling [107], general Monte Carlo methods [60], [108], and cross-entropy methods [109]–[111] have been applied to PI-based stochastic optimal control.

Various case studies of PI-based optimal control have been published [112]: autonomous driving [62], [71], [113], [114], autonomous flying [115]–[118], space robotics [73], autonomous underwater vehicles [119], and robotic manipulation planning [120], [121]. Path integral strategies for optimal predictive control have also been adopted to visual servoing techniques [113], [122]–[124]. Recently, the MPPI was integrated into Robot Operating Systems 2 (ROS 2) [125], an open-source production-grade robotics middleware framework [126].

We expect that more applications of path integral control will emerge, particularly with a focus on trajectory optimization of motion planning for autonomous systems such as mobile robots, autonomous vehicles, drones, and service robots. In addition, it has been shown that path integral control can be easily extended to the cooperative control of multi-agent systems [127]–[131].

There are still issues that must be addressed for scalable learning with safety guarantees in path integral control and its extended variations.

- Exploration-exploitation tradeoff is still not trivial,
- Comparisons of MPC-like open-loop control and parameterized state-feedback control should be further investigated, and
- Extensions to output-feedback control have not yet been studied.

The remainder of this paper is organized as follows: Section II reviews the theoretical background of path integral control and its variations. Section III describes the algorithmic implementation of several optimal control methods that employ a path-integral control framework. In Section IV, two MATLAB simulation case studies are presented to demonstrate the effectiveness of predictive path integral control. Section V presents the four ROS2/Gazebo simulation results of trajectory optimization for autonomous mobile robots, in which MPPI-based local trajectory optimization methods are demonstrated for indoor and outdoor robot navigation. In Section VI, extensions of path integral control to policy search and learning, improving sampling efficiency, multi-agent decision making, and trajectory optimization of manifolds are discussed. Section VII concludes the paper and suggests directions for future research and development of path-integral control, especially for autonomous mobile robots.

II. PATH INTEGRAL CONTROL: THEORY

A. Stochastic optimal control

Controlled stochastic differential equation Consider a controlled stochastic differential equation of the following form:

$$dX_t = f(t, X_t, \pi(t, X_t))dt + g(t, X_t, \pi(t, X_t))dW_t, \quad (1)$$

where the initial condition is given by $X_0 = x_0 \in \mathbb{R}^n$, and W_t is a standard Brownian motion. The solution to the SDE (1)

associated with the Markov policy $\pi : \mathbb{R} \times \mathbb{R}^n \rightarrow \mathbb{R}^m$ is denoted by X_t^π .

Cost-to-go function For a given Markov policy π , the cost-to-go corresponding to policy π is defined as

$$G_t^\pi = \phi(X_T^\pi) + \int_t^T L(s, X_s^\pi, \pi(s, X_s^\pi)) ds, \quad (2)$$

where $T > 0$ denotes the terminal time, $L : \mathbb{R} \times \mathbb{R}^n \times \mathbb{R}^m \rightarrow \mathbb{R}$ denotes the running cost, and $\phi : \mathbb{R}^n \rightarrow \mathbb{R}$ denotes the terminal cost.

Expected and optimal cost-to-go function The expected cost-to-go function is defined as

$$V^\pi(t, x) = \mathbb{E}[G_t^\pi | X_t^\pi = x] \quad (3)$$

where the expectation is considered with respect to the probability of the solution trajectory for the SDE (1) with an initial time and condition $(t, x) \in \mathbb{R} \times \mathbb{R}^n$. The goal of the stochastic optimal control is to determine the optimal policy.

$$\pi^* = \arg \min_{\pi} V^\pi(t, x) \quad (4)$$

The corresponding optimal cost-to-go function is defined as

$$V^*(t, x) = V^{\pi^*}(t, x) = \min_{\pi} V^\pi(t, x) \quad (5)$$

for each $(t, x) \in [0, T] \times \mathbb{R}^n$.

B. The Hamilton-Jacobi-Bellman equation

The Hamilton-Jacobi-Bellman equation for the optimal cost-to-go function is defined as follows [132]

$$\min_{\pi} \{L(t, x, \pi(t, x)) + \mathcal{T}^\pi V^*(t, x)\} = 0 \quad (6)$$

for each $(t, x) \in [0, T] \times \mathbb{R}^n$, where

$$\begin{aligned} \mathcal{T}^\pi V^*(t, x) \\ = \lim_{h \rightarrow 0+} (\mathbb{E}[V^*(t+h, X_{t+h}^\pi) | X_t^\pi = x] - V^*(t, x)) \end{aligned} \quad (7)$$

is a backward evolution operator defined on the functions of the class $\mathcal{C}^1 \times \mathcal{C}^2$. Additionally, the boundary condition is given by $V^*(T, x) = \phi(x)$.

C. Linearization of the HJB PDE

Control affine form and a quadratic cost As a special case of (1), we consider the controlled dynamics (diffusion process)

$$dX_t = f(t, X_t) dt + g(t, X_t)(\pi(t, X_t)) dt + dW_t, \quad (8)$$

and the cost-to-go

$$\begin{aligned} G_t^\pi = \phi(X_T^\pi) + \int_t^T \pi(s, X_s^\pi)^\top dW_s \\ + \int_t^T \left(q(s, X_s^\pi) + \frac{1}{2} \pi(s, X_s^\pi)^\top \pi(s, X_s^\pi) \right) ds \end{aligned} \quad (9)$$

where X_s^π is the solution to the SDE (8) for $s \in [t, T]$ with the initial condition $X_t^\pi = x_t$. In this study, we assume $G_t^\pi > 0$ for all $t \in [0, T]$ and any (control) policy π .

Remark. Notice that

1) G_t^π is not adaptive with respect to the Brownian motion as it depends on (X_τ^π) for $\tau > t$.

2) The second term in (9) is a stochastic integral with respect to the Brownian motion and it vanishes when taking expectation. This term will play an essential role when applying a change of measure. \square

The goal of stochastic optimal control for the dynamics (8) and the cost-to-go (9) is to determine an optimal policy that minimizes the expected cost-to-go with respect to the policy.

$$V^*(t, x) := \min_{\pi} \mathbb{E}[G_t^\pi | X_t^\pi = x], \quad (10)$$

$$\pi^*(t, x) := \arg \min_{\pi} V^\pi(t, x), \quad (11)$$

where the expectation \mathbb{E} is considered with respect to the stochastic process $X_{t:T}^\pi \sim \mathcal{P}^\pi$ which is the (solution) path of SDE (8).

Theorem 1: [132]–[134] The solution of the stochastic optimal control in (10) and (11) is given as

$$V^*(t, x) = -\ln \mathbb{E}\left[e^{-G_t^\pi} | X_t^\pi = x\right], \quad (12)$$

and

$$\begin{aligned} \pi^*(t, x) = \pi(t, x) \\ + \lim_{s \rightarrow t+} \frac{\mathbb{E}[(W_s - W_t)e^{-G_t^\pi} | X_t^\pi = x]}{\mathbb{E}[(s-t)e^{-G_t^\pi} | X_t^\pi = x]}, \end{aligned} \quad (13)$$

where $\pi(t, x)$ denotes an arbitrary Markov policy. \blacksquare

Because the solution represented in Theorem 1 is defined in terms of a path integral for which the expectation \mathbb{E} is taken with respect to the random process $X_{t:T}^\pi \sim \mathcal{P}^\pi$, that is, the (solution) path of the SDE (8), this class of stochastic optimal control with control-affine dynamics and quadratic control costs is called the path integral (PI) control.

Solution of the HJB equation For stochastic optimal control of the dynamics (8) and (9), the HJB equation can be rewritten as [133]

$$\min_u \left\{ q + \frac{1}{2} u^\top u + \mathcal{T}^u V^* \right\} = 0 \quad (14)$$

where

$$\mathcal{T}^u V^* = \partial_t V^* + (f + gu)^\top \partial_x V^* + \frac{1}{2} \text{Tr}(gg^\top \partial_{xx} V^*) \quad (15)$$

with the boundary condition $V^*(T, x) = \phi(x)$. In addition, the optimal state-feedback controller is given by

$$u^*(t, x) = -g(t, x)^\top \partial_x V^*(t, x). \quad (16)$$

Here, Markov policy π is replaced by state-feedback control u without loss of generality. The value (i.e., the optimal expected cost-to-go) function V^* is defined as a solution to the second-order PDE [132], [133]

$$\begin{aligned} 0 = q + \partial_t V^* - \frac{1}{2} (\partial_x V^*)^\top gg^\top \partial_x V^* + f^\top \partial_x V^* \\ + \frac{1}{2} \text{Tr}(gg^\top \partial_{xx} V^*). \end{aligned} \quad (17)$$

Linearization via exponential transformation We define an exponential transformation as follows:

$$\psi(t, x) = \exp\left(-\frac{1}{\lambda}V^*(t, x)\right) \quad (18)$$

that also belongs to class $\mathcal{C}^1 \times \mathcal{C}^2$ provided $V^*(t, x)$ does. Applying the backward evolution operator of the *uncontrolled* process, that is, $u = 0$, to the function $\psi(t, x)$, we obtain

$$\mathcal{T}^0\psi = \partial_t\psi + f^\top \partial_x\psi + \frac{1}{2}\text{Tr}(gg^\top \partial_{xx}\psi) = \frac{1}{\lambda}q\psi \quad (19)$$

which is a linear PDE with the boundary condition $\psi(T, x) = \exp(-\phi(x)/\lambda)$. This linear PDE is known as the backward Chapman-Kolmogorov PDE [133].

D. The Feynman-Kac formula

The Feynman-Kac lemma [133] provides a solution to the linear PDE (19)

$$\psi(t, x) = \mathbb{E}\left[\exp\left(\left(-\frac{1}{\lambda}\int_t^T q(s, X_s^0)ds\right)\psi(T, x_T)\right)\right] \quad (20)$$

where $\psi(T, x_T) = \exp(-\phi(x)/\lambda)$. In other words,

$$\psi(t, x) = \mathbb{E}\left[\exp\left(-\frac{1}{\lambda}G_t^0\right) | X_t^0 = x\right] \quad (21)$$

where the expectation \mathbb{E} is taken with respect to the random process $X_{t:T}^0 \sim \mathcal{P}^0$; that is, the (solution) path of the uncontrolled version of the SDE (8)

$$dX_t^0 = f(t, X_t^0)dt + g(t, X_t^0)dW_t \quad (22)$$

and the uncontrolled cost-to-go is given by

$$G_t^0 = \phi(x_T^0) + \int_t^T q(s, X_s^0)ds \quad (23)$$

which is again a nonadaptive random process. From the definition of ψ , this gives us a path-integral form for the value function:

$$V^*(t, x) = -\lambda \ln \mathbb{E}\left[\exp\left(-\frac{1}{\lambda}G_t^0\right) | X_t^0 = x\right] \quad (24)$$

$$(t, x) \in [0, T] \times \mathbb{R}^n.$$

E. Path integral for stochastic optimal control

Path integral control Although the Feynman-Kac formula presented in Section II-D provides a method to compute or approximate the value function (24), it is still not trivial to obtain an optimal Markov policy because the optimal controller in (16) is defined in terms of the gradient of V^* , not by V^* . From (16) and Theorem 1, combined with the path integral control theory [64], [128], [135]–[138], we have

$$\begin{aligned} u^*(t, x) &= -g(t, x)^\top \partial_x V^*(t, x) \\ &= g(t, x)^\top \partial_x \ln \psi(t, x) \\ &= g(t, x)^\top \lim_{s \rightarrow t+} \frac{\mathbb{E}_{\mathcal{P}^0}[\exp(-\frac{1}{\lambda}G_t^0) \int_t^s g(\tau, X_\tau)dW_\tau]}{(s-t)\mathbb{E}_{\mathcal{P}^0}[\exp(-\frac{1}{\lambda}G_t^0)]} \end{aligned} \quad (25)$$

where the initial condition is $X_t^0 = x$. This is equivalent to (13) in Theorem 1.

Information theoretic stochastic optimal control Regularized cost-to-go function

$$\mathcal{S}_t(\mathcal{P}^\pi) = G_t^0 + \lambda \ln \frac{d\mathcal{P}^\pi}{d\mathcal{P}^0} \quad (26)$$

where G_t^0 is the state-dependent cost given in (23) and $\frac{d\mathcal{P}^\pi}{d\mathcal{P}^0}$ is the Radon-Nikodym derivative¹ for the probability measures \mathcal{P}^π and \mathcal{P}^0 . Total expected cost function

$$\begin{aligned} \mathcal{V}_t(\mathcal{P}^\pi) &= \mathbb{E}_{\mathcal{P}^\pi}[\mathcal{S}_t(\mathcal{P}^\pi)] \\ &= \mathbb{E}_{\mathcal{P}^\pi}[G_t^0] + \lambda D_{\text{KL}}(\mathcal{P}^\pi \| \mathcal{P}^0) \end{aligned} \quad (27)$$

is known as the free energy of a stochastic control system [83], [132], [139], [140]. There is an additional cost term for the KL divergence between \mathcal{P}^π and \mathcal{P}^0 which we can interpret as a control cost. From Girsanov's theorem [141], [142], we obtain the following expression for the Radon-Nikodym derivative corresponding to the trajectories of the control-affine SDE (8).

$$\frac{d\mathcal{P}^\pi}{d\mathcal{P}^0} = \exp\left(\int_t^T \frac{1}{2}\|u_s\|^2 ds + u_s^\top dW_s\right) \quad (28)$$

where $u_s = \pi(s, X_s^\pi)$ is the control input and the initial condition $X_t^\pi = X_t^0 = x_t$ with an initial time $t \in [0, T]$ can be arbitrary.

The goal of KL control is to determine a probability measure that minimizes the expected total cost.

$$\mathcal{P}^* = \mathcal{P}^{\pi^*} = \arg \min_{\mathcal{P} \in \Delta^\pi} \mathcal{V}_t(\mathcal{P}) \quad (29)$$

provided $\mathcal{V}_t^* = \inf_{\mathcal{P} \in \Delta^\pi} \mathcal{V}_t(\mathcal{P})$ exists.

Theorem 2: [128], [138] The optimal regularized cost-to-go has zero variance and is the same as the expected total cost.

$$\mathcal{S}_t(\mathcal{P}^*) = \mathcal{V}_t(\mathcal{P}^*) = -\lambda \ln \mathbb{E}_{\mathcal{P}^0}[\exp(-G_t^0/\lambda)]. \quad (30)$$

which is equivalent to (24) given in Section II-D. ■

In addition, the Radon-Nikodym derivative is given by

$$\frac{d\mathcal{P}^*}{d\mathcal{P}^0} = \frac{\exp(-G_t^0/\lambda)}{\mathbb{E}_{\mathcal{P}^0}[\exp(-G_t^0/\lambda)]} \quad (31)$$

and combining (31) with the R-N derivative (28), we obtain

$$\begin{aligned} \frac{d\mathcal{P}^*}{d\mathcal{P}^\pi} &= \omega_t^\pi \\ &= \exp\left(-\int_t^T \frac{1}{2}\|u_s\|^2 ds - u_s^\top dW_s - \frac{1}{\lambda}G_t^0\right) \end{aligned} \quad (32)$$

where $u_s = \pi(s, X_s)$ is the control input following the policy $\pi : \mathbb{R} \times \mathbb{R}^n \rightarrow \mathbb{R}^m$, and ω_t^π is known as the importance weight [105], [138] that is also a random process.

¹This R-N derivative $\frac{d\mathcal{P}^\pi}{d\mathcal{P}^0}$ denotes the density of \mathcal{P}^π relative to \mathcal{P}^0 . We assume that \mathcal{P}^π is absolutely continuous with respect to \mathcal{P}^0 , denoted by $\mathcal{P}^\pi \ll \mathcal{P}^0$.

III. PATH INTEGRAL CONTROL: ALGORITHMS

A. MC integration: Model-based rollout

Let a tuple $(\Omega, \mathcal{F}, \mathcal{Q})$ be a probability space with a random variable X and consider the function $\ell(\mathbf{X}) = \int_0^T L(\mathbf{X}_t)dt$ or $\ell(X) = L(\mathbf{X}_T)$. The main idea of path integral control is to compute the expectation

$$\rho = \mathbb{E}_{\mathcal{Q}}[\ell(\mathbf{X})] \quad (33)$$

using sampling-based methods, such as Monte Carlo simulations. In principle, function $\ell : \Omega \rightarrow \mathbb{R}$ can be any arbitrary real-valued function. A well-known drawback of Monte Carlo (MC) integration is its high variance.

Importance sampling The goal of importance sampling [60], [108] in MC techniques is to minimize the variance in the MC estimation of integration, $\mathbb{E}_{\mathcal{Q}}[\ell(\mathbf{X})] = \mathbb{E}_{\mathcal{P}}[\ell(\mathbf{X}) \frac{d\mathcal{Q}}{d\mathcal{P}}]$. To reduce the variance, we want to find a probability measure \mathcal{P} on (Ω, \mathcal{F}) with which an unbiased MC estimate for ρ is given by

$$\hat{\rho}(\mathcal{P}) = \frac{1}{N_s} \sum_{i=1}^{N_s} \ell(\mathbf{X}_i) \frac{d\mathcal{Q}}{d\mathcal{P}}(\mathbf{X}_i), \quad (34)$$

where the i th sampled path \mathbf{X}_i is generated from density \mathcal{P} , denoted by $\mathbf{X}_i \sim \mathcal{P}$, for $i = 1, \dots, N_s$.

Multiple importance sampling Multiple-based probability measures can also be used for the MC estimation.

$$\hat{\rho}(\{\mathcal{P}^j\}_{j=1}^{N_p}) = \frac{1}{N} \sum_{j=1}^{N_p} \sum_{i=1}^{N_s^j} \ell(\mathbf{X}_i^j) \frac{d\mathcal{Q}}{d\mathcal{P}^j}(\mathbf{X}_i^j) \gamma^j(\mathbf{X}_i^j) \quad (35)$$

where $\mathbf{X}_i^j \sim \mathcal{P}^j$ for $i = 1, \dots, N_s^j$ and $j = 1, \dots, N_p$. Here, $N = \sum_{j=1}^{N_p} N_s^j$ is the total number of sampled paths, and the reweighting function $\gamma^j : \Omega \rightarrow \mathbb{R}$ can be any function that satisfies the relation

$$\ell(\mathbf{X}) \neq 0 \Rightarrow \frac{1}{N} \sum_{j=1}^{N_p} N_s^j \gamma^j(\mathbf{X}) = 1 \quad (36)$$

which guarantees that the resulting MC estimation $\hat{\rho}$ is unbiased [60], [61]. For example, the flat function $\gamma^j(\mathbf{X}) = 1$ for all \mathbf{X} or the balance-heuristic function $\gamma^j(\mathbf{X}) = N / \sum_{k=1}^{N_p} N_s^k \frac{d\mathcal{P}^k}{d\mathcal{P}^j}(\mathbf{X})$ can be employed [61].

B. Cross entropy method for PI: KL control

The well-known cross-entropy (CE) method [57], [60], which was originally invented for derivative-free optimization, can also be applied to trajectory generation by computing the following information theory optimization:

$$\begin{aligned} \pi^* &= \arg \min_{\pi} D_{\text{KL}}(\mathcal{P}^* \parallel \mathcal{P}^\pi) \\ &= \arg \min_{\pi} \mathbb{E}_{\mathcal{P}^*} \left[\ln \frac{d\mathcal{P}^*}{d\mathcal{P}^\pi} \right] \\ &= \arg \min_{\pi} \mathbb{E}_{\mathcal{P}^\pi} \left[\frac{d\mathcal{P}^*}{d\mathcal{P}^\pi} \ln \frac{d\mathcal{P}^*}{d\mathcal{P}^\pi} \right] \\ &= \arg \min_{\pi} \mathbb{E}_{\mathbf{X} \sim \mathcal{P}^\pi} [\omega^\pi(\mathbf{X}) \ln \omega^\pi(\mathbf{X})] \\ &= \arg \min_{\pi} \mathbb{E}_{\mathbf{X} \sim \mathcal{P}^\pi} \left[\omega^{\tilde{\pi}}(\mathbf{X}) \ln \frac{\omega^\pi(\mathbf{X})}{\omega^{\tilde{\pi}}(\mathbf{X})} \right] \\ &= \arg \min_{\pi} \mathbb{E}_{\mathbf{X} \sim \mathcal{P}^\pi} [\omega^{\tilde{\pi}}(\mathbf{X}) \ln \omega^\pi(\mathbf{X})] \end{aligned} \quad (37)$$

Algorithm 1 CE_trajopt

- 1: **Input:** K : Number of samples
 - 2: N : Decision horizon
 - 3: π^0 : Initial (trial) policy
 - 4: **while** not converged **do**
 - 5: Sample trajectories $\{\mathbf{X}_1, \dots, \mathbf{X}_K\}$ from \mathcal{P}^{π^i} .
 - 6: Determine the elite set threshold: $\gamma_i = J^{\pi^i}(\mathbf{X}_\kappa)$ where κ denotes the index of the K_e best sampled-trajectory with $K_e < K$.
 - 7: Compute the elite set of sampled-trajectories:
 - 8: $\mathcal{E}_i = \left\{ \mathbf{X}_k \mid J^{\pi^i}(\mathbf{X}_k) \leq \gamma_i \right\}$
 - 9: Update the policy:
 - 10: $\pi^{i+1} = \arg \min_{\pi} \frac{1}{|\mathcal{E}_i|} \sum_{\mathbf{X}_k \in \mathcal{E}_i} J^\pi(\mathbf{X}_k)$
 - 11: Check convergence
 - 12: **end while**
-

where the importance weight is defined as:

$$\omega^\pi(\mathbf{X}) = \frac{d\mathcal{P}^*(\mathbf{X})}{d\mathcal{P}^\pi(\mathbf{X})} = \omega^{\tilde{\pi}}(\mathbf{X}) \frac{d\mathcal{P}^{\tilde{\pi}}(\mathbf{X})}{d\mathcal{P}^\pi(\mathbf{X})} \quad (38)$$

where $\tilde{\pi}$ is the baseline Markov policy. Rewriting the cost function in the fourth row of (37) as $J^\pi(\mathbf{X}) := \omega^\pi(\mathbf{X}) \ln \omega^\pi(\mathbf{X})$, we have the following expectation minimization:

$$\min_{\pi} \mathbb{E}_{\mathbf{X} \sim \mathcal{P}^\pi} [J^\pi(\mathbf{X})]. \quad (39)$$

Algorithm 1 summarizes the iterative procedures of CE for motion planning [110] to solve the optimization problem (39) using a sampling-based method.

Remark. For expectation minimization in (39) and Algorithm 1, it is common to use a parameterization of the control policy π or the resulting trajectory distribution \mathcal{P}^π which can be rewritten as $\mathcal{P}^\pi(\mathbf{X}) = \mathcal{P}(\mathbf{X}; \theta)$. This parameterization results in a finite-dimensional optimization. \square

C. MPC-like open-loop controller: MPPI

By applying time discretization with arithmetic manipulations to (25), the path integral control becomes

$$u^*(t, x) = u(t, x) + \frac{\mathbb{E}_{\mathcal{Q}}[\exp(-\frac{1}{\lambda} G_t^\pi) \delta u]}{\mathbb{E}_{\mathcal{Q}}[\exp(-\frac{1}{\lambda} G_t^\pi)]}$$

where u is the nominal control input and δu is the deviation control input for exploration. Here, the expectation is considered with respect to the probability measure \mathcal{Q} of a path corresponding to policy π .

For implementation, the expectation is approximated using MC importance sampling as follows:

$$u^*(t, x) \approx u(t, x) + \sum_{k=1}^K \frac{\exp(-\frac{1}{\lambda} G_t^{\pi_k})}{\sum_{\kappa=1}^K \exp(-\frac{1}{\lambda} G_t^{\pi_\kappa})} \delta u_k(t, x)$$

where K is the number of sampled paths, and $G_t^{\pi_k}$ is the cost-to-go corresponding to the simulated trajectory following policy $\pi_k(t, x) = u(t, x) + \delta u_k(t, x)$ corresponding to the perturbed control inputs for $k = 1, 2, \dots, K$. This path-integral control based on forward simulations is known as

Algorithm 2 MPPI_control

```

1: Input:  $K$ : Number of samples
2:  $N$ : Decision horizon
3:  $(u_0, u_1, \dots, u_{N-1})$ : Initial control sequence
4: while not terminated do
5:   Generate random control variations  $\delta u$ 
6:   for  $k = 1, \dots, K$  do
7:      $x_0 = x_{\text{init}}$ 
8:      $t_0 = t_{\text{init}}$ 
9:     for  $i = 0, \dots, N - 1$  do
10:     $f_i = f(t_i, x_i)$ 
11:     $g_i = g(t_i, x_i)$ 
12:     $\tilde{u}_{i,k} = u_i + \delta u_{i,k}$ 
13:     $x_{i+1} = x_i + (f_i + g_i \tilde{u}_{i,k}) \Delta t$ 
14:     $t_{i+1} = t_i + \Delta t$ 
15:   end for
16:    $G_{N,k} = \text{cost}(x_N)$ 
17:   for  $i = N - 1, \dots, 0$  do
18:      $G_{i,k} = G_{i+1,k} + \text{cost}(x_i, \tilde{u}_{i,k})$ 
19:   end for
20:   end for
21:   for  $i = 0, \dots, N - 1$  do
22:      $w_{i,k} = \frac{\exp(-G_{i,k}/\lambda)}{\sum_{\kappa=1}^K \exp(-G_{i,\kappa}/\lambda)}$ 
23:      $u_i \leftarrow u_i + \sum_{k=1}^K w_{i,k} \delta u_{i,k}$ 
24:   end for
25:   Send  $u_0$  to actuators
26:   for  $i = 0, \dots, N - 1$  do
27:      $u_i = u_{\min(i+1, N-1)}$ 
28:   end for
29:   Update  $x_{\text{init}}, t_{\text{init}}$  by measurement
30: end while

```

the model-predictive path integral (MPPI) [59], [62], [64]. By recursively applying MPPI, the control inputs can approach the optimal points. Algorithm 2 summarizes the standard procedures for the MPPI.

D. Parameterized state feedback controller

Although MPC-like open-loop control methods are easy to implement, they exhibit certain limitations. First, it can be inefficient for high-dimensional control spaces because a longer horizon results in a higher dimension of the decision variables. Second, it does not design a control law (i.e., policy), but computes a sequence of control inputs over a finite horizon, which means that whenever a new state is encountered, the entire computation should be repeated. Although a warm start can help solve this problem, it remains limited. Third, the trade-off between exploitation and exploration is not trivial.

As an alternative to open-loop controller design, a parameterized policy or control law can be iteratively updated or learned via model-based rollouts, from which the performance of a candidate policy of parameterization is evaluated, and the parameters are updated to improve the control performance. The main computation procedure is that from an estimate of the probability $P(\mathbf{X}|x_0)$ of the sampled trajectories, we want to determine a parameterized policy $\pi_t(u_t|x_t; \theta_t)$ for each time

$t < T$ that can reproduce the trajectory distribution $P(\mathbf{X}|x_0)$, where $\theta_t \in \Theta$ denotes the parameter vector that defines a feedback policy π_t [58], [138]. In general, a feedback policy can be time varying, and if it is time invariant, then the time dependence can be removed; that is, $\theta = \theta_t$ for all times $t \in [0, T]$. In this review paper, we consider only deterministic feedback policies, but the main idea can be trivially extended to probabilistic feedback policies².

Linearly parameterized state feedback Consider

$$u(t, x) = h(t, x)^\top \theta \quad (40)$$

where $h : \mathbb{R} \times \mathbb{R}^n \rightarrow \mathbb{R}^{n_p}$ is a user-defined feature of the state feedback control law. Using the model-based forward simulations, a control parameter update rule can be applied as follows:

$$\theta \leftarrow \theta + \sum_{k=1}^K w_k \delta \theta_k \quad (41)$$

where $w_k = \frac{\exp(-\frac{1}{\lambda} G_t^{\pi_k})}{\sum_{\kappa=1}^K \exp(-\frac{1}{\lambda} G_t^{\pi_\kappa})}$ is the weight for the k th sampled perturbation-parameter $\delta \theta_k$ of the linearly parameterized control law and $\pi_k(t, x) = h(x, t)^\top (\theta + \delta \theta_k)$ is the test or the exploration (search) policy.

Nonlinearly parameterized state feedback Consider

$$u(t, x) = \pi(t, x; \theta) \quad (42)$$

where the state-feedback control law is parameterized by the control parameter $\theta \in \mathbb{R}^{n_p}$. Using the model-based forward simulations, a control parameter update rule can be applied as follows:

$$\theta \leftarrow \theta + \sum_{k=1}^K \tilde{w}_k \delta \theta_k \quad (43)$$

where the weight is defined as follows:

$$\tilde{w}_k = w_k [\nabla_\theta \pi(t, x; \theta)]^\dagger [\nabla_\theta \pi(t, x; \theta + \delta \theta_k)] \quad (44)$$

with the weight $w_k = \frac{\exp(-\frac{1}{\lambda} G_t^{\pi_k})}{\sum_{\kappa=1}^K \exp(-\frac{1}{\lambda} G_t^{\pi_\kappa})}$ and the exploration policy $\pi_k = \pi(t, x; \theta + \delta \theta_k)$. Here, $[\cdot]^\dagger$ denotes the pseudoinverse.

Remark (CE method for policy improvement). *Parameterized state feedback controls, such as (40) and (42), can also be updated using CE methods. For example, $\delta \theta_k \sim \mathcal{GP}(0, \Sigma)$ is samples, the cost of simulated trajectories is evaluated with control parameters $\theta_k = \theta + \delta \theta_k$ for $k = 1, \dots, K$, the samples are sorted in ascending order according to the simulated costs, and the parameter is updated by weighted-averaging the sampled parameters $\delta \theta_k$ from the sorted elite set, $\theta \leftarrow \theta + \text{average}(\delta \theta_k)_{\text{elite}}$. In general, the covariance Σ can be also updated by empirical covariance of the sampled parameters $\delta \theta_k$ from the sorted elite set, $\Sigma \leftarrow \Sigma + \text{average}(\delta \theta_k \delta \theta_k^\top)_{\text{elite}}$. \square*

²An example of probabilistic feedback policy parameterization is a time-dependent Gaussian policy that is linear in the states, $\pi_t(u_t|x_t; \theta_t) \sim \mathcal{N}(u_t|k_t + K_t x_t, S_t)$, in which the parameter vector is $\theta_t = (k_t, K_t, S_t)$ and updated by a weighted linear regression and the weighted sample-covariance matrix [58], [143].

Algorithm 3 PI²CMA

```

1: Input:  $K$ : Number of samples
2:  $N$ : Decision horizon
3:  $(\theta, \Sigma)$ : Initial hyper-parameter
4: while not terminated do
5:   Generate random variables  $\theta_{k,i} \sim \mathcal{GP}(\theta, \Sigma)$ 
6:   Generate random initial conditions  $x_{\text{init}}$ 
7:   for  $k = 1, \dots, K$  do
8:      $x_0 = x_{\text{init}}$ 
9:      $t_0 = t_{\text{init}}$ 
10:    for  $i = 0, \dots, N - 1$  do
11:       $f_i = f(t_i, x_i)$ 
12:       $g_i = g(t_i, x_i)$ 
13:       $u_{k,i} = \pi(t_i, x_i; \theta_{k,i})$ 
14:       $x_{i+1} = x_i + (f_i + g_i u_{k,i}) \Delta t$ 
15:       $t_{i+1} = t_i + \Delta t$ 
16:    end for
17:     $G_{k,N} = \text{cost}(x_N)$ 
18:    for  $i = N - 1, \dots, 0$  do
19:       $G_{k,i} = G_{k,i+1} + \text{cost}(x_i, u_{k,i})$ 
20:    end for
21:  end for
22:  for  $i = 0, \dots, N - 1$  do
23:     $w_{k,i} = \frac{\exp(-G_{k,i}/\lambda)}{\sum_{\kappa=1}^K \exp(-G_{\kappa,i}/\lambda)}$ 
24:     $\theta_i = \sum_{k=1}^K w_{k,i} \theta_{k,i}$ 
25:     $\Sigma_i = \sum_{k=1}^K w_{k,i} (\theta_{k,i} - \theta)(\theta_{k,i} - \theta)^\top$ 
26:  end for
27:   $\theta \leftarrow \sum_{i=0}^{N-1} \frac{N-i}{\sum_{j=0}^{N-1} (N-j)} \theta_i$ 
28:   $\Sigma \leftarrow \sum_{i=0}^{N-1} \frac{N-i}{\sum_{j=0}^{N-1} (N-j)} \Sigma_i$ 
29: end while

```

E. Policy improvement with path integrals

Policy improvement with path integrals (PI²) is presented in [85]. The main idea of PI² is to iteratively update the policy parameters by averaging the sampled parameters in weights with the costs of the path integral corresponding to the simulated trajectories [121]. Algorithm 3 shows the pseudocode for the PI² Covariance Matrix Adaptation (PI²-CMA) proposed in [144] based on the CMA evolutionary strategy (CMAES) [145], [146]. In [144], the PI²-CMA was compared with CE methods and CMAES in terms of optimality, exploration capability, and convergence rate. Skipping the covariance adaptation step in Algorithm 3 yields a vanilla PI². In [85], it was also shown that policy improvement methods based on PI² would outperform existing gradient-based policy search methods such as REINFORCE and NAC.

IV. MATLAB SIMULATION RESULTS

This section presents the MATLAB simulation results of the MPPI controller described in Algorithm 2 for two different trajectory optimization problems: 1D cart-pole trajectory optimization and bicycle-like mobile robot trajectory tracking. The first case study demonstrates the simulation results for the cart-pole system, followed by the second numerical experiment

showing the local trajectory tracking of a bicycle-like mobile robot with collision avoidance of dynamic obstacles. The simulation videos are publicly available³. The details of the simulation setups and numerical optimal control problems are not presented here because of limited space; however, they are available in the github page⁴.

A. Cart-pole trajectory optimization

In this section, we present the simulation results of the MPPI controller for trajectory optimization of set-point tracking in a 1D cart-pole system. The cart-pole system is a classical benchmark problem in control theory and is commonly used to evaluate the effectiveness of various control methods. To assess the performance of the MPPI controller, we conducted a series of simulations on the cart-pole system. The system consists of an inverted pendulum (pole) attached to a cart that can move along a 1D horizontal track. The objective is to stabilize the pendulum in an upright position by controlling the linear movements of the cart. We implemented the MPPI controller as described in Algorithm 2 and compared its performance with those of other state-of-the-art control algorithms commonly used for cart-pole systems.

Fig. 1 shows the controlled positions (θ, x) and velocities ($\dot{\theta}, \dot{x}$) of the cart pole system, and Fig. 2 shows the resulting force input obtained by applying the MPPI controller, whose pseudocode is presented in Algorithm 2. The performance metrics include stabilizing the pole position within a certain tolerance of the upright position and minimizing the overshoot, which measures how far the pendulum deviates from the upright position before stabilization. An animation of the cart-pole system is shown in Fig. 3 with the cart mass of 0.5 kg and list mass of 0.2 kg.

The results show that the MPPI controller can achieve the goal of stabilizing the control of the cart-pole system and maintaining the upright pole position even under varying initial conditions and in the presence of external disturbances and model uncertainties.

B. Path planning for bicycle-like mobile robot

The robot system is a mobile robot navigating an environment with obstacles, aiming to follow a predefined path while avoiding collisions. To evaluate the effectiveness of the MPPI controller for trajectory generation with obstacle avoidance, we conducted a series of simulations on a robot system. The objective was to navigate the robot along the desired path while dynamically avoiding obstacles.

We implemented the MPPI controller using Algorithm 2 for mobile robot navigation. Fig. 4 shows the robot's trajectory tracking accuracy and obstacle avoidance capabilities of the MPPI controller. Fig. 5 shows the forward and angular velocities of the robot required to follow the desired path by avoiding

³YouTube videos of the MATLAB simulation results can be found at

- <https://youtu.be/uVLMier16pc?si=K9ADCCeEqxEruF9da>
- <https://youtu.be/92BZL4yyuk8?si=MVGdhUiXJ7zI4iT1>

⁴<https://github.com/INHA-Autonomous-Systems-Laboratory-ASL/MATLAB-Simulation-An-Overview-of-Recent-Advances-in-Path-Integral-Control.git>

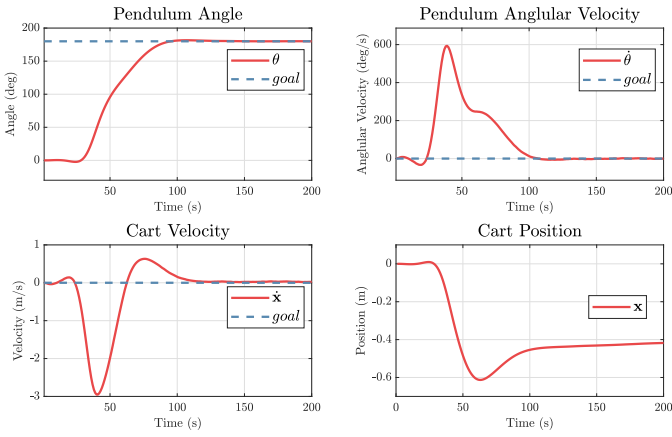


Fig. 1. Controlled trajectories of positions and velocities of the 1D cart-pole using the MPPI controller following Algorithm 2.

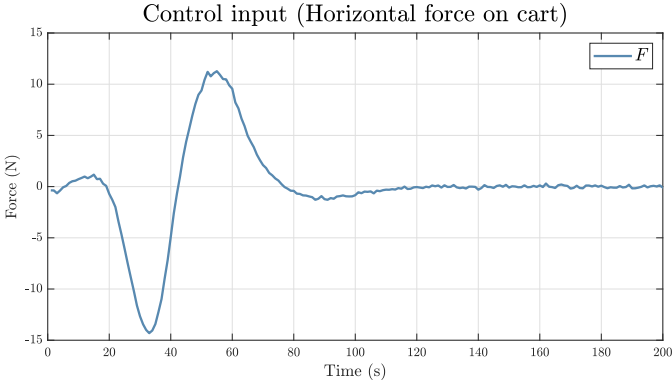


Fig. 2. Control inputs corresponding to an MPPI controller for the 1D cart-pole.

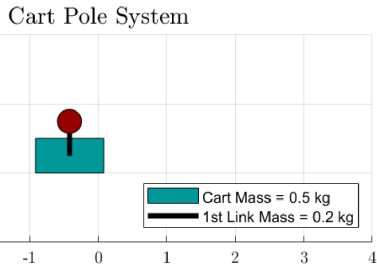


Fig. 3. A capture of controlling the 1D cart-pole. The associated animation video is available at <https://youtu.be/uVLMier16pc?si=K9ADCCeQxEruF9da>.

obstacles, which assesses the effectiveness of the controller in avoiding obstacles.

The results demonstrated that the MPPI controller achieved successful trajectory generation and tracking, while effectively avoiding dynamic obstacles. Throughout the simulation, the robot closely followed the desired path with minimal position errors. Additionally, the MPPI controller showed robust obstacle avoidance capabilities, successfully navigating around obstacles, and minimizing the number of collisions.

V. ROS2/GAZEBO SIMULATIONS FOR MPPI-BASED MOBILE ROBOT NAVIGATION

In this section, we present several ROS2/Gazebo simulations in which MPPI algorithms were applied for autonomous mobile robot navigation and control in various indoor and

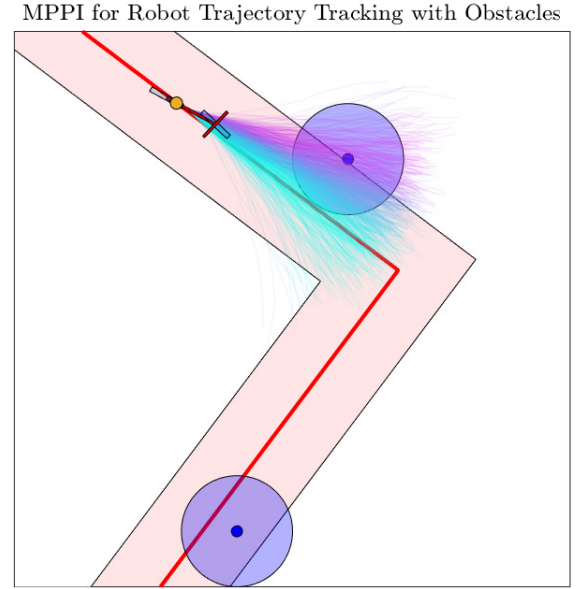


Fig. 4. A capture of local path planning and tracking with obstacle avoidance using an MPPI controller. An associated video of simulations is available at <https://youtu.be/92BZL4yyuk8?si=MVGdhUiXJ7zI4iT1>.

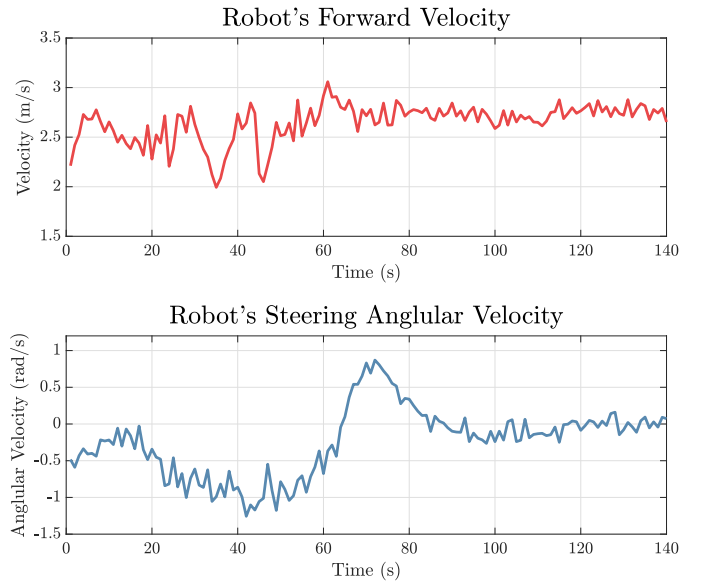


Fig. 5. Forward and angular velocity trajectories of MPPI-based controlling a bicycle-like mobile robot.

outdoor environments. The SLAM toolbox was employed for mapping while Navigation2 (NAV2) was used for navigation within the ROS2 Gazebo simulation environment [125], [126]. The MPPI approach is attractive because it is derivative-free and can be parallelized efficiently on GPU hardware. Our simulations were conducted using a computing system equipped with an Intel Core i7 CPU and a robust NVIDIA GeForce RTX 3070 GPU. These simulations were executed within Ubuntu 20.04 operating system, leveraging the ROS2-based Humble Simulation platform for comprehensive analysis. The following subsections provide the details of the simulation setups and results for the two indoor and two outdoor mobile-robot navigation scenarios. The simulation frameworks and

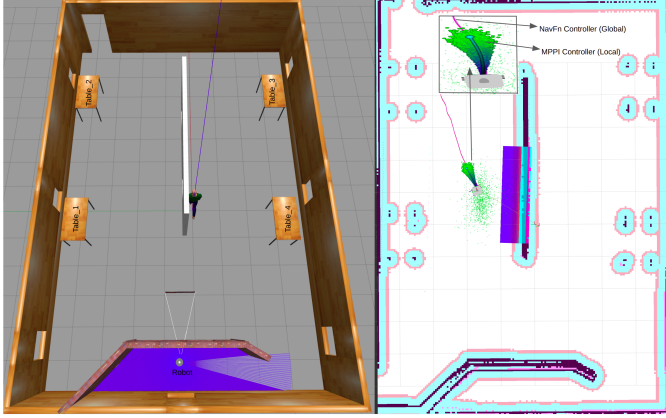


Fig. 6. MPPI-based TB3 indoor navigation in a cafeteria: Gazebo (left) and Rviz (right).

source codes used in this study are open-source⁵.

A. Turtlebot3 indoor navigation in a cafeteria

In this subsection, we present the simulation results of the Turtlebot3 (TB3) indoor navigation using an MPPI controller in a cafeteria. The primary objective of this ROS2/Gazebo simulation is to evaluate the performance of the MPPI algorithm in navigating an indoor mobile robot serving food at different tables while avoiding obstacles in a confined indoor space.

1) Experimental setup: For the indoor robot navigation scenario, we utilized a TB3 mobile robot equipped with the necessary sensors, including a LiDAR and a camera for environmental perception. The café environment was designed using Gazebo, accurately replicating the challenges of indoor navigation, including cluttered spaces, narrow passages, and dynamic moving obstacles along a path generated by a global planner, such as NavFn and Smac Hybrid-A*.

2) Simulation results: The simulation results of the TB3 navigation in a cafe environment are shown in Fig. 6 and in the accompanying video⁶, both of which illustrate the effectiveness of the MPPI controller. In the presented Gazebo simulations, the MPPI controller demonstrated remarkable indoor navigation capabilities for the differential-driving mobile robot Turtlebot3. This resulted in smooth trajectory tracking while effectively avoiding both static and dynamic obstacles in crowded café environments. The robot successfully maneuvered through tight and dense spaces while avoiding collisions with tables and other static and dynamic obstacles.

To quantitatively assess the performance, we measured key metrics, including the path-following accuracy, obstacle avoidance efficiency, and computational efficiency of the algorithm. The MPPI controller exhibited an average path-following error of less than 5% and maintained a clearance of at least 0.3 m, which is more than twice the dimension of TB3, from obstacles. The maximum linear and angular speeds were capped at 3 m/s and π rad/s, and the noise standard deviations of the control signals were 2 m/s and 2 rad/s, respectively.

⁵<https://github.com/INHA-Autonomous-Systems-Laboratory-ASL/An-Overview-on-Recent-Advances-in-Path-Integral-Control>

⁶<https://www.youtube.com/watch?v=h8smIQTszA>

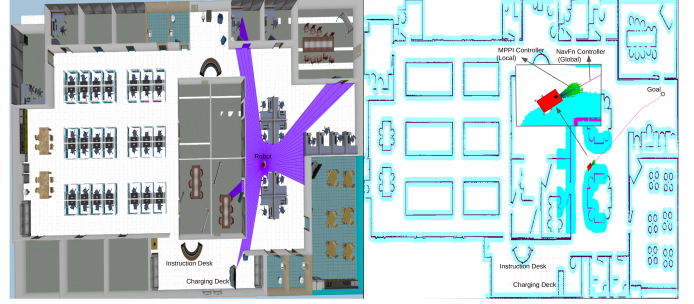


Fig. 7. MPPI-based SCOUTBOT indoor navigation in an office building: Gazebo (left) and Rviz (right).

The MPPI planners ran in a receding-horizon fashion with 100 time steps; each step was 0.1 s. The number of control rollouts was 1024 and the number of sampled traction maps was 2000 at a rate of 30 Hz. It can also replan at 30 Hz while sampling new control actions and maps. In addition, the real-time computational demands of the MPPI algorithm remained within acceptable limits for onboard embedded robot computing systems.

B. SCOUTBOT indoor navigation in an office building

In this subsection, we detail the simulation outcomes of utilizing the MPPI controller for the indoor navigation of the SCOUTBOT platform in an office environment. The objective was to gauge the efficacy of the MPPI algorithm in enabling the SCOUTBOT to navigate in a crowded environment, such as an office space, while adhering to constraints and avoiding dense obstacles.

1) Experimental setup: SCOUTBOT, equipped with LiDAR and RGB-D camera sensors, was chosen because of its adaptability and mobility. The office environment, comprising cubicles, furniture, and corridors, was simulated in a Gazebo to closely mimic the challenges posed by indoor navigation.

2) Simulation results: The MPPI-controlled SCOUTBOT demonstrated efficient indoor navigation skills. This algorithm facilitates agile traversal through an office environment and successfully circumvents tight corners, open office areas, and office furniture. Dynamic obstacles representing moving colleagues were effectively avoided. Fig. 7 and a simulation video⁷ demonstrate the efficacy of the MPPI controller in navigating the SCOUTBOT office.

The quantitative evaluation revealed encouraging outcomes. The average path deviation from the intended trajectory was maintained below 5%, whereas the SCOUTBOT consistently maintained a safety margin of 0.25 m from obstacles. The maximum linear and angular speeds were capped at 5 m/s and π rad/s, and the noise standard deviations for the control signals were 2 m/s and 2 rad/s respectively. The MPPI planners ran in a receding-horizon fashion with 100 time steps; each step was 0.1 s. The number of control rollouts was 1024, and the number of sampled traction maps was 2000 at a rate of 30 Hz. It could also replan at 30 Hz while sampling new control actions and maps. The computational overhead of the

⁷<https://youtu.be/wjBnMZDOxTg?si=XWwNZfKXRloxJD3b>

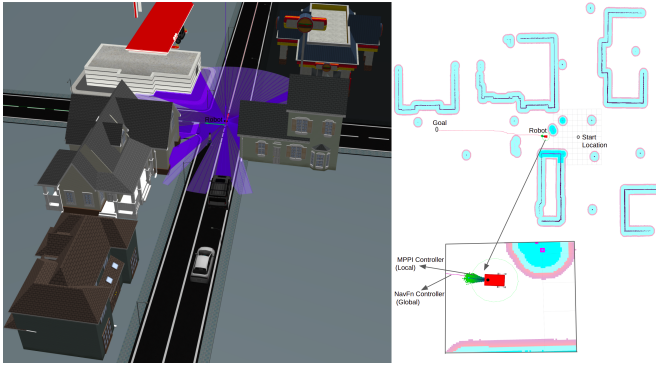


Fig. 8. MPPI-based SCOUTBOT outdoor navigation in an urban road: Gazebo (left) and Rviz (right).

MPPI algorithm remained reasonable, thereby ensuring real-time feasibility for practical applications.

C. SCOUTBOT outdoor navigation in road environment

In this subsection, we elaborate the simulation results of employing the MPPI controller for the outdoor navigation of SCOUTBOT in a road environment. Leveraging ROS2 and Gazebo, we aimed to assess the SCOUTBOT’s ability to navigate amidst vehicular traffic, adhering to road rules and ensuring pedestrian safety.

1) *Experimental setup:* The SCOUTBOT sensor suite was augmented to include additional sensors crucial for outdoor environments, such as LiDAR, cameras, and GPS. The simulated traffic environment featured roads, intersections, and pedestrian walkways and introduced complex dynamics and motion patterns.

2) *Simulation results:* The MPPI-controlled SCOUTBOT navigated outdoor roads and traffic scenarios in-depth. This demonstrates the capacity to interpret and respond to follow a defined trajectory, yield to vehicles, and avoid pedestrians. This algorithm enables a robot to make calculated decisions for lane changes and turns, showcasing its potential for safe and rule-compliant outdoor navigation. Fig. 8 and a simulation video⁸ display SCOUTBOT’s navigation in a road environment, illustrating the MPPI controller’s effectiveness.

The quantitative assessment displayed promising performance metrics. The SCOUTBOT adhered to traffic rules with a success rate exceeding 90%, while maintaining an average lateral deviation of less than 0.3 meters from its intended path. The maximum linear and angular speeds were capped at 7 m/s and π rad/s and the noise standard deviations of the control signals were 2 m/s and 2 rad/s, respectively. The MPPI planners ran in a receding-horizon fashion with 100 time steps; each step was 0.1 s. The number of control rollouts was 1024, and the number of sampled traction maps was 2000 at a rate of 30 Hz. It could also replan at 30 Hz while sampling new control actions and maps. The computational load of the MPPI algorithm remained manageable, underscoring its applicability in real-time outdoor robotic operations.

⁸<https://youtu.be/-0lAy3pWi2s?si=C29mhsaX6ORUUUVBN>

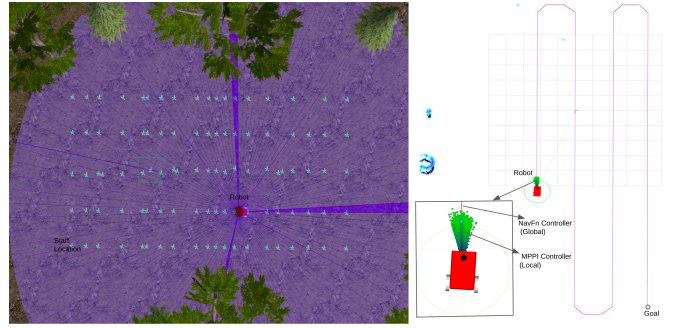


Fig. 9. MPPI-based SCOUTBOT outdoor navigation in a farm: Gazebo (left) and Rviz (right).

D. SCOUTBOT outdoor navigation in a farming area

In this subsection, we provide insights into the simulation results of utilizing the MPPI controller for the outdoor navigation of the SCOUTBOT in a farming environment. Using ROS2 and Gazebo, we aimed to evaluate the performance of the MPPI controller using SCOUTBOT to navigate through agricultural fields while considering terrain and crop boundaries.

1) *Experimental setup:* The SCOUTBOT sensor suite was enhanced to include specialized sensors such as LiDAR. The simulated farm environment encompassed uneven terrain, crop rows, and irrigation ditches, presenting challenges that are unique to agricultural settings.

2) *Simulation results:* The MPPI-controlled SCOUTBOT exhibited proficient navigation skills in farm environments. It successfully traversed rough and varying terrain, maintained alignment with the crop rows, and avoided collisions with obstacles. The robot’s ability to adapt to an unstructured outdoor environment was evident. Fig. 9 and a simulation video⁹ illustrate SCOUTBOT’s effective navigation in a farm environment using the MPPI controller.

The quantitative evaluation showed encouraging outcomes. SCOUTBOT consistently achieved an alignment accuracy of over 90% with crop rows and maintained safe trajectory tracking. The maximum linear and angular speeds were capped at 5 m/s and π rad/s, respectively, and the noise standard deviations for the control signals were 2 m/s and 2 rad/s. The MPPI planners ran in a receding-horizon fashion with 100 time steps; each step was 0.1 s. The number of control rollouts was 1024, and the number of sampled traction maps was 2000 at a rate of 30 Hz. It could also replan at 30 Hz while sampling new control actions and maps. The computational efficiency of the MPPI algorithm remained viable, demonstrating its suitability for real-time navigation and data collection for agricultural applications.

In summary, the simulation results across diverse scenarios underscore the effectiveness and versatility of the MPPI controller in enabling precise and adaptive robotic navigation. The controller exhibited the capability to handle intricate indoor, road traffic, and outdoor environments while maintaining safety, accuracy, and computational efficiency. These findings

⁹<https://youtu.be/isU3rQ82oE0?si=wzHJGyUtNb8pe-WX>

provide a solid foundation for the practical implementation of MPPI-based navigation systems on real-world robotic platforms.

VI. DISCUSSION AND FUTURE DIRECTIONS

A. Policy parameterization

There are multiple ways of policy parameterizations for state-feedback [147]. For example, linear policies [147], [148], radial basis function (RBF) networks [147]–[150], and dynamic movement primitives (DMPs) [151], [152] have been commonly used for policy representations and search in robotics and control.

Note that because the PI-based control and planning algorithms presented in Section III are derivative-free, complex policy parameterizations can be implemented without any additional effort (e.g., numerical differentiation computing gradients, Jacobians, and Hessians). This is one of the advantageous characteristics of sampling-based policy search and improvement methods such as PI.

B. Path integral for guided policy search

The guided policy search (GPS), first proposed in [86], is a model-free policy-based reinforcement learning (RL). Pixel-to-torque end-to-end learning of visuomotor policies has recently become popular for RL in robotics [153]. Compared with direct deep reinforcement learning, GPS has several advantages, such as faster convergence and better optimality. In the GPS, learning consists of two phases. The first phase involves determining a local guiding policy, in which a training set of controlled trajectories is generated. In the second phase, a complex global policy is determined via supervised learning, in which the expected KL divergence of the global policy from the guiding policy is minimized. The goal of the GPS framework is to solve an information-theoretic-constrained optimization of the following [87]:

$$\begin{aligned} & \min_{\theta, \beta} \mathbb{E}_{\beta}[G(\mathbf{X})] \\ & \text{s.t. } D_{\text{KL}}(\beta(\mathbf{X}) \| \pi(\mathbf{X}; \theta)) \leq \epsilon \end{aligned} \quad (45)$$

where the KL divergence $D_{\text{KL}}(\beta(\mathbf{X}) \| \pi(\mathbf{X}; \theta))$ can be rewritten as:

$$\sum_{i=0}^{N-1} \mathbb{E}_{\beta}[D_{\text{KL}}(\beta(u_i|x_i) \| \pi(u_i|x_i; \theta))].$$

A baseline (Markovian) policy $\beta(u_i|x_i)$ is a local guiding policy used to generate sampled trajectories starting with a variety of initial conditions. A parameterized policy $\pi(u_i|x_i; \theta)$ is a high-dimensional global policy learned based on the sampled trajectories generated from the baseline policy β in a supervisory manner by minimizing the KL divergence from the local policy.

The iterative procedure for a general GPS is summarized as follows. (*Step 1*) Given $\hat{\theta}$, solve

$$\begin{aligned} \hat{\beta} &= \arg \min_{\beta} \mathbb{E}_{\beta}[G(\mathbf{X})] \\ &\text{s.t. } D_{\text{KL}}(\beta(\mathbf{X}) \| \pi(\mathbf{X}; \hat{\theta})) \leq \epsilon. \end{aligned}$$

(*Step 2*) Given $\hat{\beta}$, solve

$$\hat{\theta} = \arg \min_{\theta} D_{\text{KL}}(\hat{\beta}(\mathbf{X}) \| \pi(\mathbf{X}; \theta)).$$

(*Step 3*) Check convergence and repeat Steps 1 and 2 until a convergence criterion is met.

Various methods have been considered to guide GPS policies. For example, gradient-based local optimal control methods such as DDP and iLQR and sampling-based local approximate optimal control methods such as PI and PI² can be used. Among others, we claim that because of their efficiency in exploration and fast convergence rate, PI-based sampling methods could be more appropriate as guiding policies for GPS.

C. Sampling efficiency for variance reduction

Let us consider the importance weight defined in (38). Note that if the training policy π is optimal, then all simulated trajectories have the same weight. To measure the quality of the sampling strategy, the effective sampling size (ESS) defined as

$$\text{ESS}^{\pi} = \frac{1}{\mathbb{E}_{\mathcal{P}^{\pi}}[(\omega^{\pi})^2]} \quad (46)$$

measures the variance of the importance weights and can be used to quantify the efficiency of a sampling method [154], [155]. A small ESS implies that the associated back-end tasks of estimation or control may result in a large variance. The most important sampling strategies suffer from decreasing ESS over time during prediction. Therefore, quantifying or approximating the ESS of a base-sampling strategy is a major problem in the application of path integral control [138], [156].

D. Extensions to multi-agent systems

In the literature, there are only a few studies that extend PI control to the stochastic control of multi-agent systems: path integrals for centralized control [129], distributed control [130], [131], and a two-player zero-sum stochastic differential game (SDG) [157].

In path planning and control for multi-agent systems, it is common to assume that dynamics are independent but costs are interdependent. Consider the cost-to-go function defined for agent a as

$$G_{a,t}^{\bar{\pi}^a} = \phi_a(\bar{X}_{a,T}^{\bar{\pi}^a}) + \int_t^T L(s, \bar{X}_{a,s}^{\bar{\pi}^a}, \bar{\pi}_a(s, \bar{X}_{a,s}^{\bar{\pi}^a})) ds,$$

where $\bar{\pi}_a = (\pi_a, \pi_{\nu(a)})$ is the joint policy of the ego agent a and its neighbourhood agent $\nu(a)$. Similarly the joint state and trajectory are defined as $\bar{X}_{a,s} = (X_{a,s}, X_{\nu(a),s})$ and $\bar{X}_{a,t} = (\bar{X}_{a,s})_{s=t}^T = (X_{a,s}, X_{\nu(a),s})_s^T$.

As we have observed throughout this paper for single-agent cases, from an algorithmic point of view, the most important computation is to approximate the weights corresponding to the likelihood ratios using MC sampling methods. Similarly, policy updates or improvements in multi-agent systems can be

$$\pi_a \leftarrow \pi_a + \sum_{k=1}^K \hat{w}_{a,k}^{\bar{\pi}^a} \delta \pi_{a,k}$$

where the probability weight is defined as

$$\hat{w}_{a,k}^{\bar{\pi}_a} = \frac{\exp\left(-\frac{1}{\lambda}G_{a,t}^{(\bar{\pi}_{a,k}, \bar{\pi}_{\nu(a)})}\right)}{\sum_{\kappa=1}^K \exp\left(-\frac{1}{\lambda}G_{a,t}^{(\bar{\pi}_{a,\kappa}, \bar{\pi}_{\nu(a)})}\right)}$$

for which randomly perturbed policies $\bar{\pi}_{a,k} = \pi_a + \delta\pi_{a,k}$ are used to simulate the controlled trajectories and compute the associated costs $G_{a,t}^{(\bar{\pi}_{a,k}, \bar{\pi}_{\nu(a)})}$. Here, the learning process is assumed to be asynchronous, in the sense that the policies of the neighborhood agents $\nu(a)$ are fixed when updating the policy for agent a in accordance with the simulation of the augmented trajectories \bar{X}_a . Here, the individual agent's policy can be either MPC-like open-loop (feedforward) control inputs or parameterized (deterministic or stochastic) state-feedback controllers.

E. MPPI for trajectory optimization on manifolds

Trajectory optimization using differential geometry is very common in robotics and has been studied under manifolds such as special orthogonal and Euclidean groups $\text{SO}(3)$ and $\text{SE}(3)$ [158]–[161]. In [159], gradient-based sequential convex programming on manifolds was used for trajectory optimization. It was expected that many theoretical and computational frameworks for the optimization of manifolds [162], [163] could be applied to robotic trajectory optimization.

Applying methods of sampling-based path integral control such as MPPI to trajectory optimization on manifolds is not trivial because it requires effective accelerated approaches to generate the sampled trajectories on manifolds and sampling trajectories on manifolds with kinematic constraints are not trivial. Thus, one could employ the methods used for unscented Kalman filtering on manifolds (UKF-M) [164]–[167]. We leave this research topic of sampling-based path integral control for trajectory optimization on manifolds for potential future work.

VII. CONCLUSIONS

In this paper, we present an overview of the fundamental theoretical developments and recent advances in path integral control with a focus on sampling-based stochastic trajectory optimization. The theoretical and algorithmic frameworks of several optimal control methods employing the path integral control framework are provided, and their similarities and differences are reviewed. MATLAB and ROS2/Gazebo simulation results are provided to demonstrate the effectiveness of MPPI control, which is the most popular method for path integral control. Discussions on policy parameterization and optimization in policy search adopting path integral control, efficiency sampling strategies, extending the path integral control framework to multi-agent optimal control problems, and path integral control for the trajectory optimization of manifolds are provided. We expect that sampling-based stochastic trajectory optimization employing path integral control can be applied to practical engineering problems, particularly for agile mobile robot navigation and control.

REFERENCES

- [1] O. Von Stryk and R. Bulirsch, “Direct and indirect methods for trajectory optimization,” *Annals of operations research*, vol. 37, no. 1, pp. 357–373, 1992.
- [2] J. T. Betts, “Survey of numerical methods for trajectory optimization,” *Journal of guidance, control, and dynamics*, vol. 21, no. 2, pp. 193–207, 1998.
- [3] A. V. Rao, “Trajectory optimization: A survey,” *Optimization and optimal control in automotive systems*, pp. 3–21, 2014.
- [4] H. Choset, K. M. Lynch, S. Hutchinson, G. A. Kantor, and W. Burgard, *Principles of robot motion: theory, algorithms, and implementations*. MIT press, 2005.
- [5] J.-C. Latombe, *Robot motion planning*. Springer Science & Business Media, 2012, vol. 124.
- [6] S. M. LaValle, *Planning algorithms*. Cambridge university press, 2006.
- [7] B. Paden, M. Čáp, S. Z. Yong, D. Yershov, and E. Frazzoli, “A survey of motion planning and control techniques for self-driving urban vehicles,” *IEEE Transactions on Intelligent Vehicles*, vol. 1, no. 1, pp. 33–55, 2016.
- [8] L. Claussmann, M. Revilloud, D. Gruyer, and S. Glaser, “A review of motion planning for highway autonomous driving,” *IEEE Transactions on Intelligent Transportation Systems*, vol. 21, no. 5, pp. 1826–1848, 2019.
- [9] S. Teng, X. Hu, P. Deng, B. Li, Y. Li, Y. Ai, D. Yang, L. Li, Z. Xuanyuan, F. Zhu *et al.*, “Motion planning for autonomous driving: The state of the art and future perspectives,” *IEEE Transactions on Intelligent Vehicles*, 2023.
- [10] Y. Song, M. Steinweg, E. Kaufmann, and D. Scaramuzza, “Autonomous drone racing with deep reinforcement learning,” in *2021 IEEE/RSJ International Conference on Intelligent Robots and Systems (IROS)*. IEEE, 2021, pp. 1205–1212.
- [11] Z. Han, Z. Wang, N. Pan, Y. Lin, C. Xu, and F. Gao, “Fast-Racing: An open-source strong baseline for $\text{se}(3)$ planning in autonomous drone racing,” *IEEE Robotics and Automation Letters*, vol. 6, no. 4, pp. 8631–8638, 2021.
- [12] D. Hanover, A. Loquercio, L. Bauersfeld, A. Romero, R. Penicka, Y. Song, G. Cioffi, E. Kaufmann, and D. Scaramuzza, “Autonomous drone racing: A survey,” *arXiv e-prints*, pp. arXiv–2301, 2023.
- [13] M. Lan, S. Lai, T. H. Lee, and B. M. Chen, “A survey of motion and task planning techniques for unmanned multicopter systems,” *Unmanned Systems*, vol. 9, no. 02, pp. 165–198, 2021.
- [14] M. Wang, J. Diepolder, S. Zhang, M. Söpper, and F. Holzapfel, “Trajectory optimization-based maneuverability assessment of evtol aircraft,” *Aerospace Science and Technology*, vol. 117, p. 106903, 2021.
- [15] J. Park, I. Kim, J. Suk, and S. Kim, “Trajectory optimization for takeoff and landing phase of uam considering energy and safety,” *Aerospace Science and Technology*, vol. 140, p. 108489, 2023.
- [16] P. Pradeep, T. A. Lauderdale, G. B. Chatterji, K. Sheth, C. F. Lai, B. Sridhar, K.-M. Edholm, and H. Erzberger, “Wind-optimal trajectories for multirotor evtol aircraft on uam missions,” in *Aiaa Aviation 2020 Forum*, 2020, p. 3271.
- [17] H.-H. Kwon and H.-L. Choi, “A convex programming approach to mid-course trajectory optimization for air-to-ground missiles,” *International Journal of Aeronautical and Space Sciences*, vol. 21, pp. 479–492, 2020.
- [18] H. Roh, Y.-J. Oh, M.-J. Tahk, K.-J. Kwon, and H.-H. Kwon, “L1 penalized sequential convex programming for fast trajectory optimization: With application to optimal missile guidance,” *International Journal of Aeronautical and Space Sciences*, vol. 21, pp. 493–503, 2020.
- [19] I. Garcia and J. P. How, “Trajectory optimization for satellite reconfiguration maneuvers with position and attitude constraints,” in *Proceedings of the 2005, American Control Conference, 2005*. IEEE, 2005, pp. 889–894.
- [20] A. Weiss, F. Leve, M. Baldwin, J. R. Forbes, and I. Kolmanovsky, “Spacecraft constrained attitude control using positively invariant constraint admissible sets on $\text{SO}(3) \times \mathbb{R}^3$,” in *2014 American Control Conference*. IEEE, 2014, pp. 4955–4960.
- [21] A. Gatherer and Z. Manchester, “Magnetorquer-only attitude control of small satellites using trajectory optimization,” in *Proceedings of AAS/AIAA Astrodynamics Specialist Conference*, 2019.
- [22] D. Malyuta, Y. Yu, P. Elango, and B. Açıkmese, “Advances in trajectory optimization for space vehicle control,” *Annual Reviews in Control*, vol. 52, pp. 282–315, 2021.

- [23] T. L. Dearing, J. Hauser, X. Chen, M. M. Nicotra, and C. Petersen, "Efficient trajectory optimization for constrained spacecraft attitude maneuvers," *Journal of Guidance, Control, and Dynamics*, vol. 45, no. 4, pp. 638–650, 2022.
- [24] J. Canny, *The complexity of robot motion planning*. MIT press, 1988.
- [25] M. Elbanhawi and M. Simic, "Sampling-based robot motion planning: A review," *IEEE Access*, vol. 2, pp. 56–77, 2014.
- [26] Z. Kingston, M. Moll, and L. E. Kavraki, "Sampling-based methods for motion planning with constraints," *Annual review of control, robotics, and autonomous systems*, vol. 1, no. 1, pp. 159–185, 2018.
- [27] J. T. Betts, *Practical methods for optimal control and estimation using nonlinear programming*. Philadelphia, PA: SIAM, 2010.
- [28] M. Kelly, "An introduction to trajectory optimization: How to do your own direct collocation," *SIAM Review*, vol. 59, no. 4, pp. 849–904, 2017.
- [29] R. Bonalli, A. Cauligi, A. Bylard, and M. Pavone, "GuSTO: Guaranteed sequential trajectory optimization via sequential convex programming," in *2019 International conference on robotics and automation (ICRA)*. IEEE, 2019, pp. 6741–6747.
- [30] T. A. Howell, B. E. Jackson, and Z. Manchester, "ALTRO: A fast solver for constrained trajectory optimization," in *2019 IEEE/RSJ International Conference on Intelligent Robots and Systems (IROS)*. IEEE, 2019, pp. 7674–7679.
- [31] S. G. Manyam, D. W. Casbeer, I. E. Weintraub, and C. Taylor, "Trajectory optimization for rendezvous planning using quadratic Bézier curves," in *2021 IEEE/RSJ International Conference on Intelligent Robots and Systems (IROS)*. IEEE, 2021, pp. 1405–1412.
- [32] D. Malyuta, T. P. Reynolds, M. Szmułek, T. Lew, R. Bonalli, M. Pavone, and B. Açıkmese, "Convex optimization for trajectory generation: A tutorial on generating dynamically feasible trajectories reliably and efficiently," *IEEE Control Systems Magazine*, vol. 42, no. 5, pp. 40–113, 2022.
- [33] D. H. Jacobson and D. Q. Mayne, *Differential dynamic programming*. Elsevier Publishing Company, 1970, no. 24.
- [34] D. Q. Mayne, "Differential dynamic programming—a unified approach to the optimization of dynamic systems," in *Control and dynamic systems*. Elsevier, 1973, vol. 10, pp. 179–254.
- [35] Z. Xie, C. K. Liu, and K. Hauser, "Differential dynamic programming with nonlinear constraints," in *2017 IEEE International Conference on Robotics and Automation (ICRA)*. IEEE, 2017, pp. 695–702.
- [36] J. Chen, W. Zhan, and M. Tomizuka, "Autonomous driving motion planning with constrained iterative LQR," *IEEE Transactions on Intelligent Vehicles*, vol. 4, no. 2, pp. 244–254, 2019.
- [37] A. Pavlov, I. Shames, and C. Manzie, "Interior point differential dynamic programming," *IEEE Transactions on Control Systems Technology*, vol. 29, no. 6, pp. 2720–2727, 2021.
- [38] K. Cao, M. Cao, S. Yuan, and L. Xie, "DIRECT: A differential dynamic programming based framework for trajectory generation," *IEEE Robotics and Automation Letters*, vol. 7, no. 2, pp. 2439–2446, 2022.
- [39] I. Chatzinikolaidis and Z. Li, "Trajectory optimization of contact-rich motions using implicit differential dynamic programming," *IEEE Robotics and Automation Letters*, vol. 6, no. 2, pp. 2626–2633, 2021.
- [40] M.-G. Kim and K.-K. K. Kim, "An extension of interior point differential dynamic programming for optimal control problems with second-order cone constraints," *Transactions of the Korean Institute of Electrical Engineers*, vol. 71, no. 11, pp. 1666–1672, 2022.
- [41] X. Zhong, J. Tian, H. Hu, and X. Peng, "Hybrid path planning based on safe a* algorithm and adaptive window approach for mobile robot in large-scale dynamic environment," *Journal of Intelligent & Robotic Systems*, vol. 99, no. 1, pp. 65–77, 2020.
- [42] S. Sun, A. Romero, P. Foehn, E. Kaufmann, and D. Scaramuzza, "A comparative study of nonlinear MPC and differential-flatness-based control for quadrotor agile flight," *IEEE Transactions on Robotics*, vol. 38, no. 6, pp. 3357–3373, 2022.
- [43] M. Faessler, A. Franchi, and D. Scaramuzza, "Differential flatness of quadrotor dynamics subject to rotor drag for accurate tracking of high-speed trajectories," *IEEE Robotics and Automation Letters*, vol. 3, no. 2, pp. 620–626, 2017.
- [44] A. Domahidi and J. Jerez, "FORCES Professional," EmbotechAG, url=<https://embotech.com/FORCES-Pro>, 2014–2023.
- [45] J. D. Gammell and M. P. Strub, "Asymptotically optimal sampling-based motion planning methods," *arXiv preprint arXiv:2009.10484*, 2020.
- [46] J. J. Kuffner and S. M. LaValle, "RRT-connect: An efficient approach to single-query path planning," in *2000 IEEE International Conference on Robotics and Automation (ICRA)*, vol. 2. IEEE, 2000, pp. 995–1001.
- [47] L. Janson, B. Ichter, and M. Pavone, "Deterministic sampling-based motion planning: Optimality, complexity, and performance," *The International Journal of Robotics Research*, vol. 37, no. 1, pp. 46–61, 2018.
- [48] L. Campos-Macías, D. Gómez-Gutiérrez, R. Aldana-López, R. de la Guardia, and J. I. Parra-Vilchis, "A hybrid method for online trajectory planning of mobile robots in cluttered environments," *IEEE Robotics and Automation Letters*, vol. 2, no. 2, pp. 935–942, 2017.
- [49] A. A. Ravankar, A. Ravankar, T. Emara, and Y. Kobayashi, "HPPRM: Hybrid potential based probabilistic roadmap algorithm for improved dynamic path planning of mobile robots," *IEEE Access*, vol. 8, pp. 221743–221766, 2020.
- [50] F. Kiani, A. Seyyedabbasi, R. Aliyev, M. U. Gulle, H. Basyildiz, and M. A. Shah, "Adapted-RRT: Novel hybrid method to solve three-dimensional path planning problem using sampling and metaheuristic-based algorithms," *Neural Computing and Applications*, vol. 33, no. 22, pp. 15 569–15 599, 2021.
- [51] Z. Yu, Z. Si, X. Li, D. Wang, and H. Song, "A novel hybrid particle swarm optimization algorithm for path planning of uavs," *IEEE Internet of Things Journal*, vol. 9, no. 22, pp. 22 547–22 558, 2022.
- [52] I. A. Sucan, M. Moll, and L. E. Kavraki, "The open motion planning library," *IEEE Robotics & Automation Magazine*, vol. 19, no. 4, pp. 72–82, 2012.
- [53] M. Kalakrishnan, S. Chitta, E. Theodorou, P. Pastor, and S. Schaal, "STOMP: Stochastic trajectory optimization for motion planning," in *2011 IEEE international conference on robotics and automation*. IEEE, 2011, pp. 4569–4574.
- [54] M. Likhachev, "Search-based planning lab," 2010. [Online]. Available: <http://sbpl.net/Home>
- [55] M. Zucker, N. Ratliff, A. D. Dragan, M. Pivtoraiko, M. Klingensmith, C. M. Dellin, J. A. Bagnell, and S. S. Srinivasa, "Chomp: Covariant hamiltonian optimization for motion planning," *The International Journal of Robotics Research*, vol. 32, no. 9–10, pp. 1164–1193, 2013.
- [56] H. J. Kappen, "Linear theory for control of nonlinear stochastic systems," *Physical review letters*, vol. 95, no. 20, p. 200201, 2005.
- [57] R. Y. Rubinstein and D. P. Kroese, *The cross-entropy method: A unified approach to combinatorial optimization, Monte-Carlo simulation, and machine learning*. Springer, 2004, vol. 133.
- [58] V. Gómez, H. J. Kappen, J. Peters, and G. Neumann, "Policy search for path integral control," in *Joint European Conference on Machine Learning and Knowledge Discovery in Databases*. Springer, 2014, pp. 482–497.
- [59] G. Williams, A. Aldrich, and E. A. Theodorou, "Model predictive path integral control: From theory to parallel computation," *Journal of Guidance, Control, and Dynamics*, vol. 40, no. 2, pp. 344–357, 2017.
- [60] R. Y. Rubinstein and D. P. Kroese, *Simulation and the Monte Carlo method*. John Wiley & Sons, 2016.
- [61] S. Thijssen and H. Kappen, "Consistent adaptive multiple importance sampling and controlled diffusions," *arXiv preprint arXiv:1803.07966*, 2018.
- [62] G. Williams, P. Drews, B. Goldfain, J. M. Rehg, and E. A. Theodorou, "Aggressive driving with model predictive path integral control," in *2016 IEEE International Conference on Robotics and Automation (ICRA)*. IEEE, 2016, pp. 1433–1440.
- [63] ———, "Information-theoretic model predictive control: Theory and applications to autonomous driving," *IEEE Transactions on Robotics*, vol. 34, no. 6, pp. 1603–1622, 2018.
- [64] G. R. Williams, "Model predictive path integral control: Theoretical foundations and applications to autonomous driving," Ph.D. dissertation, Georgia Institute of Technology, 2019.
- [65] Y. Pan, E. Theodorou, and M. Kontitsis, "Sample efficient path integral control under uncertainty," *Advances in Neural Information Processing Systems*, vol. 28, 2015.
- [66] I. Abraham, A. Handa, N. Ratliff, K. Lowrey, T. D. Murphrey, and D. Fox, "Model-based generalization under parameter uncertainty using path integral control," *IEEE Robotics and Automation Letters*, vol. 5, no. 2, pp. 2864–2871, 2020.
- [67] J. Pravitra, K. A. Ackerman, C. Cao, N. Hovakimyan, and E. A. Theodorou, "L1-Adaptive MPPI architecture for robust and agile control of multirotors," in *2020 IEEE/RSJ International Conference on Intelligent Robots and Systems (IROS)*, 2020, pp. 7661–7666.
- [68] G. Williams, E. Rombokas, and T. Daniel, "GPU based path integral control with learned dynamics," *arXiv preprint arXiv:1503.00330*, 2015.

- [69] M. Okada, T. Aoshima, and L. Rigazio, "Path integral networks: End-to-end differentiable optimal control," *arXiv preprint arXiv:1706.09597*, 2017.
- [70] I. S. Mohamed, M. Ali, and L. Liu, "GP-guided MPPI for efficient navigation in complex unknown cluttered environments," *arXiv preprint arXiv:2307.04019*, 2023.
- [71] M. S. Gandhi, B. Vlahov, J. Gibson, G. Williams, and E. A. Theodorou, "Robust model predictive path integral control: Analysis and performance guarantees," *IEEE Robotics and Automation Letters*, vol. 6, no. 2, pp. 1423–1430, 2021.
- [72] E. Arruda, M. J. Mathew, M. Kopicki, M. Mistry, M. Azad, and J. L. Wyatt, "Uncertainty averse pushing with model predictive path integral control," in *2017 IEEE-RAS 17th International Conference on Humanoid Robotics (Humanoids)*. IEEE, 2017, pp. 497–502.
- [73] M. Raisi, A. Noohian, and S. Fallah, "A fault-tolerant and robust controller using model predictive path integral control for free-flying space robots," *Frontiers in Robotics and AI*, vol. 9, p. 1027918, 2022.
- [74] J. Zeng, B. Zhang, and K. Sreenath, "Safety-critical model predictive control with discrete-time control barrier function," in *2021 American Control Conference (ACC)*. IEEE, 2021, pp. 3882–3889.
- [75] C. Tao, H.-J. Yoon, H. Kim, N. Hovakimyan, and P. Voulgaris, "Path integral methods with stochastic control barrier functions," in *2022 IEEE 61st Conference on Decision and Control (CDC)*. IEEE, 2022, pp. 1654–1659.
- [76] J. Yin, C. Dawson, C. Fan, and P. Tsotras, "Shield model predictive path integral: A computationally efficient robust MPC approach using control barrier functions," *arXiv preprint arXiv:2302.11719*, 2023.
- [77] J. Yin, Z. Zhang, E. Theodorou, and P. Tsotras, "Trajectory distribution control for model predictive path integral control using covariance steering," in *2022 International Conference on Robotics and Automation (ICRA)*. IEEE, 2022, pp. 1478–1484.
- [78] F. S. Barbosa, B. Lacerda, P. Duckworth, J. Tumova, and N. Hawes, "Risk-aware motion planning in partially known environments," in *2021 60th IEEE Conference on Decision and Control (CDC)*. IEEE, 2021, pp. 5220–5226.
- [79] Z. Wang, O. So, K. Lee, and E. A. Theodorou, "Adaptive risk sensitive model predictive control with stochastic search," in *Learning for Dynamics and Control*. PMLR, 2021, pp. 510–522.
- [80] X. Cai, M. Everett, L. Sharma, P. R. Osteen, and J. P. How, "Probabilistic traversability model for risk-aware motion planning in off-road environments," *arXiv preprint arXiv:2210.00153*, 2022.
- [81] J. Yin, Z. Zhang, and P. Tsotras, "Risk-aware model predictive path integral control using conditional value-at-risk," in *2023 IEEE International Conference on Robotics and Automation (ICRA)*. IEEE, 2023, pp. 7937–7943.
- [82] C. Tao, H. Kim, and N. Hovakimyan, "RRT guided model predictive path integral method," *arXiv preprint arXiv:2301.13143*, 2023.
- [83] E. A. Theodorou and E. Todorov, "Relative entropy and free energy dualities: Connections to path integral and KL control," in *2012 51st IEEE Conference on Decision and Control (CDC)*. IEEE, 2012, pp. 1466–1473.
- [84] A. Ijspeert, J. Nakanishi, and S. Schaal, "Learning attractor landscapes for learning motor primitives," *Advances in neural information processing systems*, vol. 15, 2002.
- [85] E. Theodorou, J. Buchli, and S. Schaal, "A generalized path integral control approach to reinforcement learning," *The Journal of Machine Learning Research*, vol. 11, pp. 3137–3181, 2010.
- [86] S. Levine and V. Koltun, "Guided policy search," in *International Conference on Machine Learning*. PMLR, 2013, pp. 1–9.
- [87] W. H. Montgomery and S. Levine, "Guided policy search via approximate mirror descent," *Advances in Neural Information Processing Systems (NIPS)*, vol. 29, 2016.
- [88] M.-G. Kim and K.-K. K. Kim, "MPPI-IPDDP: Hybrid method of collision-free smooth trajectory generation for autonomous robots," *arXiv preprint arXiv:2208.02439*, 2022.
- [89] D. Thalmeier, H. J. Kappen, S. Totaro, and V. Gómez, "Adaptive smoothing for path integral control," *The Journal of Machine Learning Research*, vol. 21, no. 1, pp. 7814–7850, 2020.
- [90] S. Särkkä, "Unscented rauch–tung–striebel smoother," *IEEE transactions on automatic control*, vol. 53, no. 3, pp. 845–849, 2008.
- [91] H.-C. Ruiz and H. J. Kappen, "Particle smoothing for hidden diffusion processes: Adaptive path integral smoother," *IEEE Transactions on Signal Processing*, vol. 65, no. 12, pp. 3191–3203, 2017.
- [92] T. Neve, T. Lefebvre, and G. Crevecoeur, "Comparative study of sample based model predictive control with application to autonomous racing," in *2022 IEEE/ASME International Conference on Advanced Intelligent Mechatronics (AIM)*. IEEE, 2022, pp. 1632–1638.
- [93] T. Kim, G. Park, K. Kwak, J. Bae, and W. Lee, "Smooth model predictive path integral control without smoothing," *IEEE Robotics and Automation Letters*, vol. 7, no. 4, pp. 10406–10413, 2022.
- [94] T. Lefebvre and G. Crevecoeur, "Entropy regularised deterministic optimal control: From path integral solution to sample-based trajectory optimisation," in *2022 IEEE/ASME International Conference on Advanced Intelligent Mechatronics (AIM)*. IEEE, 2022, pp. 401–408.
- [95] A. Lambert, A. Fishman, D. Fox, B. Boots, and F. Ramos, "Stein variational model predictive control," *arXiv preprint arXiv:2011.07641*, 2020.
- [96] B. Eysenbach and S. Levine, "If MaxEnt RL is the answer, what is the question?" *arXiv preprint arXiv:1910.01913*, 2019.
- [97] P. Whittle, "Likelihood and cost as path integrals," *Journal of the Royal Statistical Society: Series B (Methodological)*, vol. 53, no. 3, pp. 505–529, 1991.
- [98] H. J. Kappen, V. Gómez, and M. Opper, "Optimal control as a graphical model inference problem," *Machine learning*, vol. 87, no. 2, pp. 159–182, 2012.
- [99] J. Watson, H. Abdulsamad, and J. Peters, "Stochastic optimal control as approximate input inference," in *Conference on Robot Learning*. PMLR, 2020, pp. 697–716.
- [100] T. Haarnoja, H. Tang, P. Abbeel, and S. Levine, "Reinforcement learning with deep energy-based policies," in *International conference on machine learning*. PMLR, 2017, pp. 1352–1361.
- [101] S. Levine, "Reinforcement learning and control as probabilistic inference: Tutorial and review," *arXiv preprint arXiv:1805.00909*, 2018.
- [102] L. Martino, V. Elvira, D. Luengo, and J. Corander, "An adaptive population importance sampler: Learning from uncertainty," *IEEE Transactions on Signal Processing*, vol. 63, no. 16, pp. 4422–4437, 2015.
- [103] S. U. Stich, A. Raj, and M. Jaggi, "Safe adaptive importance sampling," *Advances in Neural Information Processing Systems*, vol. 30, 2017.
- [104] M. F. Bugallo, V. Elvira, L. Martino, D. Luengo, J. Miguez, and P. M. Djuric, "Adaptive importance sampling: The past, the present, and the future," *IEEE Signal Processing Magazine*, vol. 34, no. 4, pp. 60–79, 2017.
- [105] H. J. Kappen and H. C. Ruiz, "Adaptive importance sampling for control and inference," *Journal of Statistical Physics*, vol. 162, no. 5, pp. 1244–1266, 2016.
- [106] D. M. Asmar, R. Senanayake, S. Manuel, and M. J. Kochenderfer, "Model predictive optimized path integral strategies," in *2023 IEEE International Conference on Robotics and Automation (ICRA)*, 2023, pp. 3182–3188.
- [107] J. Carius, R. Ranftl, F. Farshidian, and M. Hutter, "Constrained stochastic optimal control with learned importance sampling: A path integral approach," *The International Journal of Robotics Research*, vol. 41, no. 2, pp. 189–209, 2022.
- [108] B. Arouna, "Adaptive Monte Carlo method, a variance reduction technique," *Monte Carlo Methods and Applications*, vol. 10, no. 1, pp. 1–24, 2004.
- [109] P.-T. De Boer, D. P. Kroese, S. Mannor, and R. Y. Rubinstein, "A tutorial on the cross-entropy method," *Annals of operations research*, vol. 134, no. 1, pp. 19–67, 2005.
- [110] M. Kobilarov, "Cross-entropy motion planning," *The International Journal of Robotics Research*, vol. 31, no. 7, pp. 855–871, 2012.
- [111] W. Zhang, H. Wang, C. Hartmann, M. Weber, and C. Schute, "Applications of the cross-entropy method to importance sampling and optimal control of diffusions," *SIAM Journal on Scientific Computing*, vol. 36, no. 6, pp. A2654–A2672, 2014.
- [112] M. Testouri, G. Elghazaly, and R. Frank, "Towards a safe real-time motion planning framework for autonomous driving systems: An MPPI approach," *arXiv preprint arXiv:2308.01654*, 2023.
- [113] I. S. Mohamed, K. Yin, and L. Liu, "Autonomous navigation of AGVs in unknown cluttered environments: log-MPPI control strategy," *IEEE Robotics and Automation Letters*, vol. 7, no. 4, pp. 10240–10247, 2022.
- [114] J.-S. Ha, S.-S. Park, and H.-L. Choi, "Topology-guided path integral approach for stochastic optimal control in cluttered environment," *Robotics and Autonomous Systems*, vol. 113, pp. 81–93, 2019.
- [115] I. S. Mohamed, G. Allibert, and P. Martinet, "Model predictive path integral control framework for partially observable navigation: A quadrotor case study," in *2020 16th International Conference on Control, Automation, Robotics and Vision (ICARCV)*. IEEE, 2020, pp. 196–203.
- [116] J. Pravitra, E. Theodorou, and E. N. Johnson, "Flying complex maneuvers with model predictive path integral control," in *AIAA Scitech 2021 Forum*, 2021, p. 1957.

- [117] M. D. Houghton, A. B. Oshin, M. J. Acheson, E. A. Theodorou, and I. M. Gregory, "Path planning: Differential dynamic programming and model predictive path integral control on VTOL aircraft," in *AIAA SCITECH 2022 Forum*, 2022, p. 0624.
- [118] J. Higgins, N. Mohammad, and N. Bezzo, "A model predictive path integral method for fast, proactive, and uncertainty-aware UAV planning in cluttered environments," *arXiv preprint arXiv:2308.00914*, 2023.
- [119] P. Nicolay, Y. Petillot, M. Marfeychuk, S. Wang, and I. Carlacho, "Enhancing AUV autonomy with model predictive path integral control," *arXiv preprint arXiv:2308.05547*, 2023.
- [120] L. Hou, H. Wang, H. Zou, and Y. Zhou, "Robotic manipulation planning for automatic peeling of glass substrate based on online learning model predictive path integral," *Sensors*, vol. 22, no. 3, p. 1292, 2022.
- [121] K. Yamamoto, R. Ariizumi, T. Hayakawa, and F. Matsuno, "Path integral policy improvement with population adaptation," *IEEE Transactions on Cybernetics*, vol. 52, no. 1, pp. 312–322, 2020.
- [122] I. S. Mohamed, G. Allibert, and P. Martinet, "Sampling-based MPC for constrained vision based control," in *2021 IEEE/RSJ International Conference on Intelligent Robots and Systems (IROS)*. IEEE, 2021, pp. 3753–3758.
- [123] I. S. Mohamed, "MPPI-VS: Sampling-based model predictive control strategy for constrained image-based and position-based visual servoing," *arXiv preprint arXiv:2104.04925*, 2021.
- [124] M. Costanzo, G. De Maria, C. Natale, and A. Russo, "Modeling and control of sampled-data image-based visual servoing with three-dimensional features," *IEEE Transactions on Control Systems Technology*, 2023, (Early Access).
- [125] S. Macenski, T. Moore, D. V. Lu, A. Merzlyakov, and M. Ferguson, "From the desks of ROS maintainers: A survey of modern & capable mobile robotics algorithms in the robot operating system 2," *Robotics and Autonomous Systems*, p. 104493, 2023.
- [126] S. Macenski, T. Foote, B. Gerkey, C. Lalancette, and W. Woodall, "Robot operating system 2: Design, architecture, and uses in the wild," *Science Robotics*, vol. 7, no. 66, p. eabm6074, 2022.
- [127] B. Van Den Broek, W. Wiegerinck, and B. Kappen, "Graphical model inference in optimal control of stochastic multi-agent systems," *Journal of Artificial Intelligence Research*, vol. 32, pp. 95–122, 2008.
- [128] S. A. Thijssen, "Path integral control," Ph.D. dissertation, Radboud University, 2016.
- [129] V. Gómez, S. Thijssen, A. Symington, S. Hailes, and H. J. Kappen, "Real-time stochastic optimal control for multi-agent quadrotor systems," in *Proceedings of the Twenty-Sixth International Conference on Automated Planning and Scheduling (ICAPS)*, 2016, pp. 468–476.
- [130] N. Wan, A. Gahlawat, N. Hovakimyan, E. A. Theodorou, and P. G. Voulgaris, "Cooperative path integral control for stochastic multi-agent systems," in *2021 American Control Conference (ACC)*. IEEE, 2021, pp. 1262–1267.
- [131] P. Varnai and D. V. Dimarogonas, "Multi-agent stochastic control using path integral policy improvement," in *2022 American Control Conference*, 2022.
- [132] W. H. Fleming and H. M. Soner, *Controlled Markov processes and viscosity solutions*. Springer Science & Business Media, 2006, vol. 25.
- [133] B. Oksendal, *Stochastic differential equations: an introduction with applications*. Springer Science & Business Media, 2013.
- [134] W. H. Fleming and R. W. Rishel, *Deterministic and stochastic optimal control*. Springer Science & Business Media, 2012, vol. 1.
- [135] H. J. Kappen, "An introduction to stochastic control theory, path integrals and reinforcement learning," in *AIP Conference Proceedings*, vol. 887, no. 1. American Institute of Physics, 2007, pp. 149–181.
- [136] H. Kappen, "Optimal control theory and the linear bellman equation," *Barber, D.; Cemgil, AT; Chiappa, S.(ed.), Bayesian time series models*, pp. 363–387, 2011.
- [137] E. A. Theodorou, "Iterative path integral stochastic optimal control: Theory and applications to motor control," Ph.D. dissertation, University of Southern California, 2011.
- [138] S. Thijssen and H. Kappen, "Path integral control and state-dependent feedback," *Physical Review E*, vol. 91, no. 3, p. 032104, 2015.
- [139] W. H. Fleming and W. M. McEneaney, "Risk-sensitive control on an infinite time horizon," *SIAM Journal on Control and Optimization*, vol. 33, no. 6, pp. 1881–1915, 1995.
- [140] E. A. Theodorou, "Nonlinear stochastic control and information theoretic dualities: Connections, interdependencies and thermodynamic interpretations," *Entropy*, vol. 17, no. 5, pp. 3352–3375, 2015.
- [141] R. S. Liptser and A. N. Shiryaev, *Statistics of random processes: General theory*. Springer, 1977, vol. 394.
- [142] R. S. Liptser and A. N. Shiryaev, *Statistics of random processes II: Applications*. Springer Science & Business Media, 2013, vol. 6.
- [143] A. Kupcsik, M. Deisenroth, J. Peters, and G. Neumann, "Data-efficient contextual policy search for robot movement skills," in *Proceedings of the National Conference on Artificial Intelligence (AAAI)*. Bellevue, 2013.
- [144] F. Stulp and O. Sigaud, "Path integral policy improvement with covariance matrix adaptation," *arXiv preprint arXiv:1206.4621*, 2012.
- [145] N. Hansen and A. Ostermeier, "Completely derandomized self-adaptation in evolution strategies," *Evolutionary Computation*, vol. 9, no. 2, pp. 159–195, 2001.
- [146] N. Hansen, "The CMA evolution strategy: A tutorial," *arXiv preprint arXiv:1604.00772*, 2016.
- [147] M. P. Deisenroth, G. Neumann, J. Peters *et al.*, "A survey on policy search for robotics," *Foundations and Trends® in Robotics*, vol. 2, no. 1–2, pp. 1–142, 2013.
- [148] J. Vinogradskaya, B. Bischoff, J. Achterhold, T. Koller, and J. Peters, "Numerical quadrature for probabilistic policy search," *IEEE Transactions on Pattern Analysis and Machine Intelligence*, vol. 42, no. 1, pp. 164–175, 2020.
- [149] M. P. Deisenroth, D. Fox, and C. E. Rasmussen, "Gaussian processes for data-efficient learning in robotics and control," *IEEE Transactions on Pattern Analysis and Machine Intelligence*, vol. 37, no. 2, pp. 408–423, 2013.
- [150] M. Thor, T. Kulvicius, and P. Manoonpong, "Generic neural locomotion control framework for legged robots," *IEEE Transactions on Neural Networks and Learning Systems*, vol. 32, no. 9, pp. 4013–4025, 2020.
- [151] S. Schaal, J. Peters, J. Nakanishi, and A. Ijspeert, "Learning movement primitives," in *Robotics research. the eleventh international symposium*. Springer, 2005, pp. 561–572.
- [152] A. J. Ijspeert, J. Nakanishi, H. Hoffmann, P. Pastor, and S. Schaal, "Dynamical movement primitives: Learning attractor models for motor behaviors," *Neural computation*, vol. 25, no. 2, pp. 328–373, 2013.
- [153] S. Levine, C. Finn, T. Darrell, and P. Abbeel, "End-to-end training of deep visuomotor policies," *The Journal of Machine Learning Research*, vol. 17, no. 1, pp. 1334–1373, 2016.
- [154] J. H. Kotecha and P. M. Djuric, "Gaussian sum particle filtering," *IEEE Transactions on signal processing*, vol. 51, no. 10, pp. 2602–2612, 2003.
- [155] J. S. Liu, *Monte Carlo strategies in scientific computing*. Springer, 2001, vol. 75.
- [156] Q. Zhang and Y. Chen, "Path integral sampler: A stochastic control approach for sampling," in *International Conference on Learning Representations*, 2022.
- [157] A. Patil, Y. Zhou, D. Fridovich-Keil, and T. Tanaka, "Risk-minimizing two-player zero-sum stochastic differential game via path integral control," *arXiv preprint arXiv:2308.11546*, 2023.
- [158] M. Watterson, S. Liu, K. Sun, T. Smith, and V. Kumar, "Trajectory optimization on manifolds with applications to $\text{SO}(3)$ and $\mathbb{R}^3 \times \mathbb{S}^2$," in *Robotics: Science and Systems*, 2018, p. 9.
- [159] R. Bonalli, A. Bylard, A. Cauligi, T. Lew, and M. Pavone, "Trajectory optimization on manifolds: A theoretically-guaranteed embedded sequential convex programming approach," *arXiv preprint arXiv:1905.07654*, 2019.
- [160] M. Watterson, S. Liu, K. Sun, T. Smith, and V. Kumar, "Trajectory optimization on manifolds with applications to quadrotor systems," *The International Journal of Robotics Research*, vol. 39, no. 2-3, pp. 303–320, 2020.
- [161] T. Osa, "Motion planning by learning the solution manifold in trajectory optimization," *The International Journal of Robotics Research*, vol. 41, no. 3, pp. 281–311, 2022.
- [162] N. Boumal, B. Mishra, P.-A. Absil, and R. Sepulchre, "Manopt, a Matlab toolbox for optimization on manifolds," *The Journal of Machine Learning Research*, vol. 15, no. 1, pp. 1455–1459, 2014.
- [163] N. Boumal, *An introduction to optimization on smooth manifolds*. Cambridge University Press, 2023.
- [164] H. M. Menegaz, J. Y. Ishihara, and H. T. Kussaba, "Unscented Kalman filters for Riemannian state-space systems," *IEEE Transactions on Automatic Control*, vol. 64, no. 4, pp. 1487–1502, 2018.
- [165] M. Brossard, A. Barrau, and S. Bonnabel, "A code for unscented Kalman filtering on manifolds (UKF-M)," in *2020 IEEE International Conference on Robotics and Automation (ICRA)*. IEEE, 2020, pp. 5701–5708.
- [166] K. Li, F. Pfaff, and U. D. Hanebeck, "Unscented dual quaternion particle filter for $\text{SE}(3)$ estimation," *IEEE Control Systems Letters*, vol. 5, no. 2, pp. 647–652, 2020.

- [167] T. Cantelobre, C. Chahbazian, A. Croux, and S. Bonnabel, “A real-time unscented Kalman filter on manifolds for challenging AUV navigation,” in *2020 IEEE/RSJ International Conference on Intelligent Robots and Systems (IROS)*. IEEE, 2020, pp. 2309–2316.